

Pharmacokinetic Parameter	Geometric Mean			Point Estimate (90% C.I.)
Atazanavir				
	Day 6	Day 10	Day 21	Day 10/Day 6 Ratio
C _{max} (ng/mL)	5135.62	5420.97	--	1.06 (0.93, 1.20) ✓
AUC(TAU) (ng·h/mL) ^a	29493.64	37889.89	--	1.28 (1.16, 1.43)
Clarithromycin				
	Day 6	Day 10	Day 21	Day 10/Day 21 Ratio
C _{max} (ng/mL)	--	3574.96	2375.65	1.50 (1.32, 1.71)
AUC(TAU) (ng·h/mL) ^b	--	34847.08	17916.62	1.94 (1.75, 2.16)
14-OH Clarithromycin				
	Day 6	Day 10	Day 21	Day 10/Day 21 Ratio
C _{max} (ng/mL)	--	209.72	746.83	0.28 (0.24, 0.33)
AUC(TAU) (ng·h/mL) ^b	--	2044.59	6898.35	0.30 (0.26, 0.34)

Treatment: Atazanavir at 400 mg QD for 6 days (Days 1-6) followed by co-administration of atazanavir at 400 mg QD and clarithromycin at 500 mg BID for 4 days (Days 7-10). Washout of 7 days (Days 11-17) followed by administration of clarithromycin at 500 mg BID for 4 days (Days 18-21)

^a TAU = 12 h

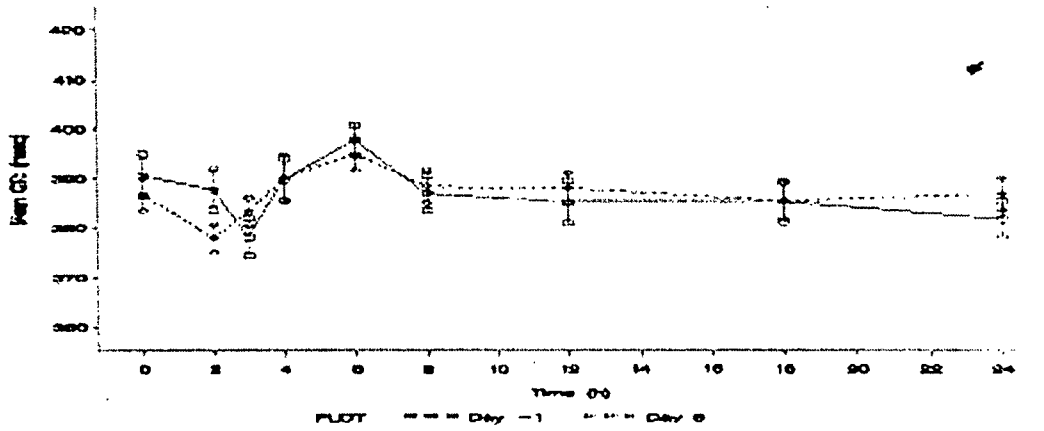
^b TAU = 24 h

The increase of approximately 30% in atazanavir exposure upon co-administration with clarithromycin occurred presumably as a result of inhibition of clearance rather than an increase in bioavailability, as the T-HALF of atazanavir was enhanced relative to atazanavir administered alone. Similarly, the increase of approximately 100% in clarithromycin exposure appeared to occur due to an inhibition of clearance rather than to an increase in bioavailability, as the T-HALF of clarithromycin doubled. Accordingly, there was a marked decrease in exposure of 14-OH clarithromycin, which is formed by CYP3A-mediated metabolism. The sponsor suggested a reduction in clarithromycin dose to 250 mg BID when co-administered with atazanavir at 400 mg QD.

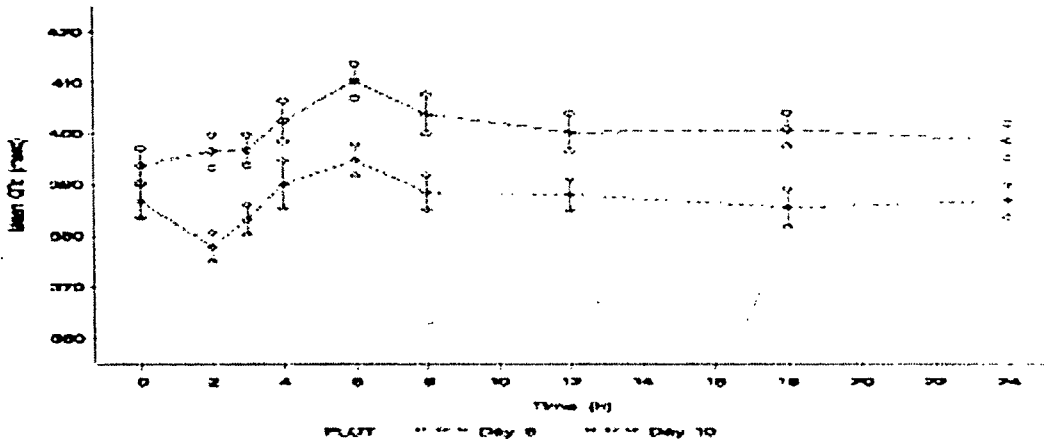
Reviewer's comment: The metabolite of clarithromycin, 14-OH clarithromycin, has been reported to have some antimicrobial activity, but is not significant for Mycobacterium avium complex (MAC). Therefore, the applicant proposed dose regimen is acceptable for MAC but not for other indications. Consider alternative therapy for indications other than infections due to MAC.

QTc (Bazett's correction)

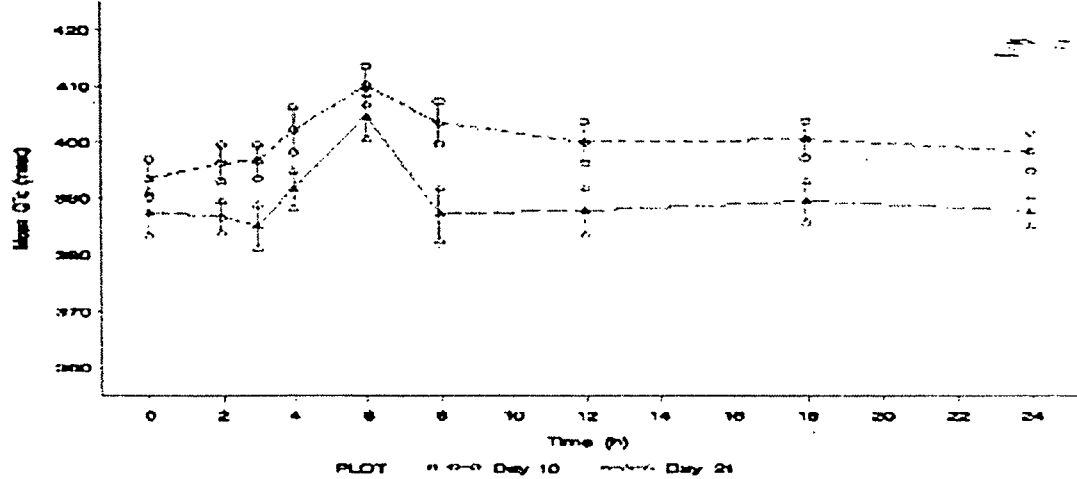
Plot of Mean QTc versus Time on Days -1 and 6



Plot of Mean QTc versus Time on Days 6 and 10



Plot of Mean QTc versus Time on Days 10 and 21



The results showed that clarithromycin and atazanavir, when co-administered together, have additive effects on the QTc interval, as compared to the effect due to administration of atazanavir or clarithromycin alone. The summary statistics for change from baseline QTc Max to QTc Max are presented in the following table.

	Study Day		
	Day 6 (n = 29)	Day 10 (n = 29)	Day 21 (n = 21)
Δ_1 QTc Max (msec) Mean (S.D.)	14 (13)	30 (19)	19 (16)

The following two tables also showed that there were more subjects with borderline QTc prolongation and abnormal QTc changes from baseline when atazanavir and clarithromycin were coadministered as compared to either drug alone.

Listing of Subjects with Borderline QTc Intervals

Subject	Gender	Study Day	Time Point	QTc (msec)
002	Male	21	6 h	432
007	Male	4	Pre-Dose	436
016	Male	10	8 h	445
021	Male	10	6 h	436
023	Female	6	4 h	461
028	Female	10	8 h	452
		Discharge	48 h post-dose	473

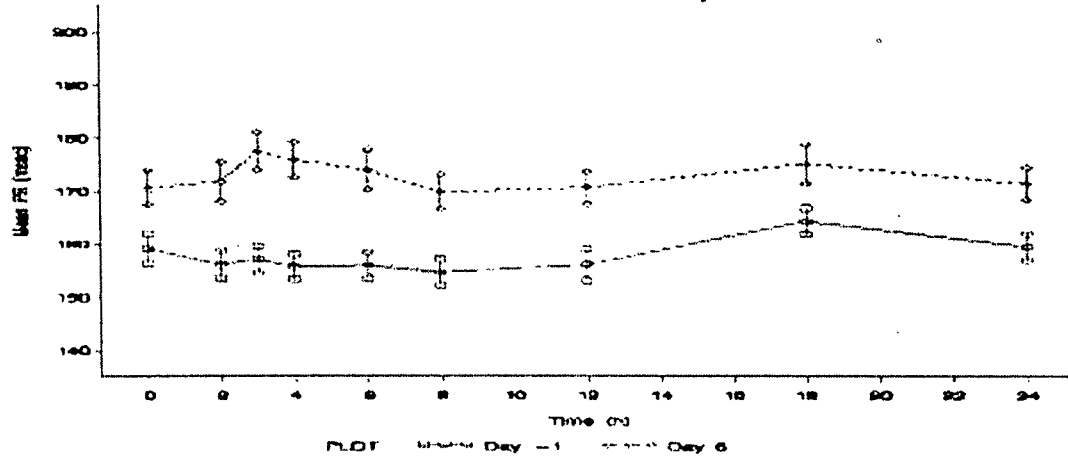
Counts of Subjects with different severity of QTc Changes from Baseline

Study Day	Gender	QTc Changes from Baseline (msec)		
		< 30	30-60	> 60
		Count (%)	Count (%)	Count (%)
6	Male	13 (68%)	6 (32%)	0 (0%)
	Female	6 (60%)	4 (40%)	0 (0%)
10	Male	5 (26%)	11 (58%)	3 (16%)
	Female	3 (30%)	6 (60%)	1 (10%)
21	Male	6 (38%)	9 (56%)	1 (6%)
	Female	2 (30%)	2 (40%)	1 (20%)

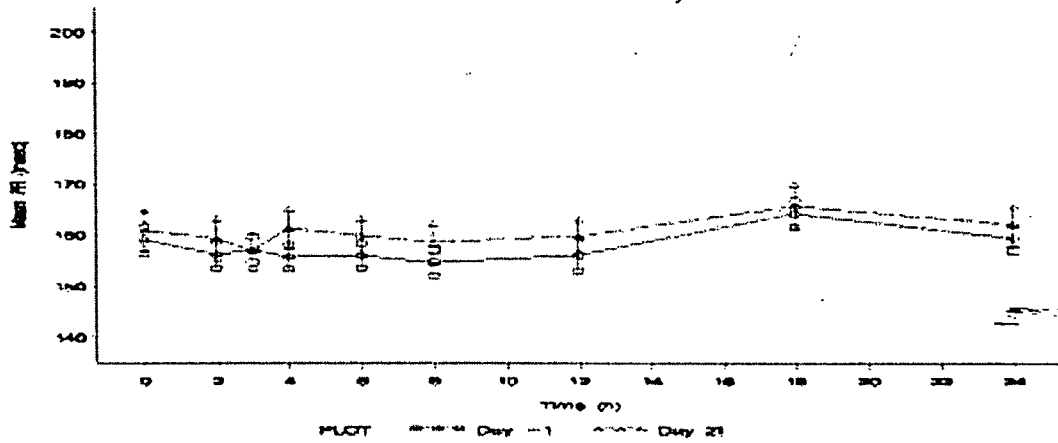
The increased clarithromycin exposure in the presence of atazanavir may partially contribute to the increased QTc prolongation when clarithromycin is combined with atazanavir. However, all QTc calculations are based on Bazett's correction, and as indicated in the review for Study AI424076, Fridericia's formulation (QTcF) is more accurate in subjects with high heart rates, it is difficult to assess the true impact of combination of atazanavir and clarithromycin.

PR

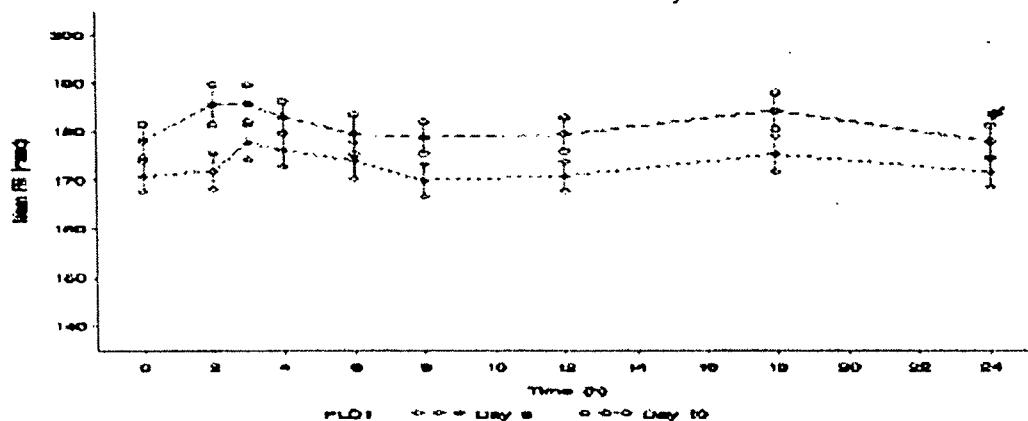
Plot of Mean PR versus Time on Days -1 and 6



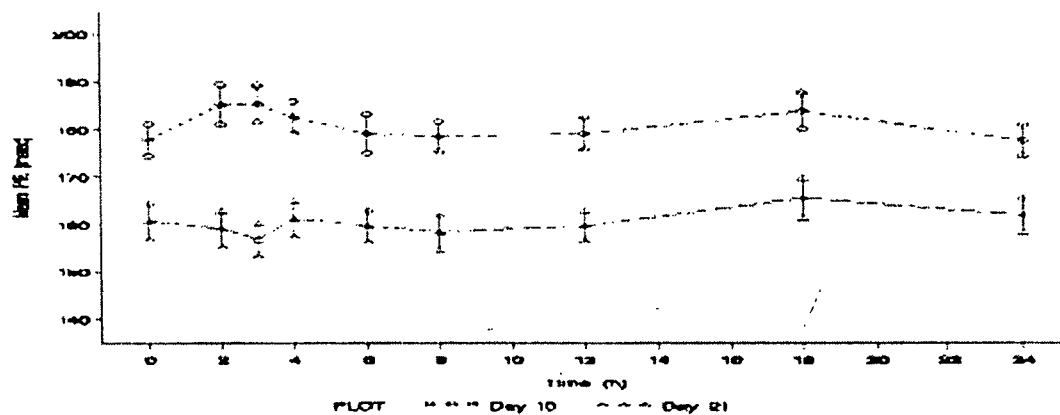
Plot of Mean PR versus Time on Days -1 and 21



Plot of Mean PR versus Time on Days 6 and 10



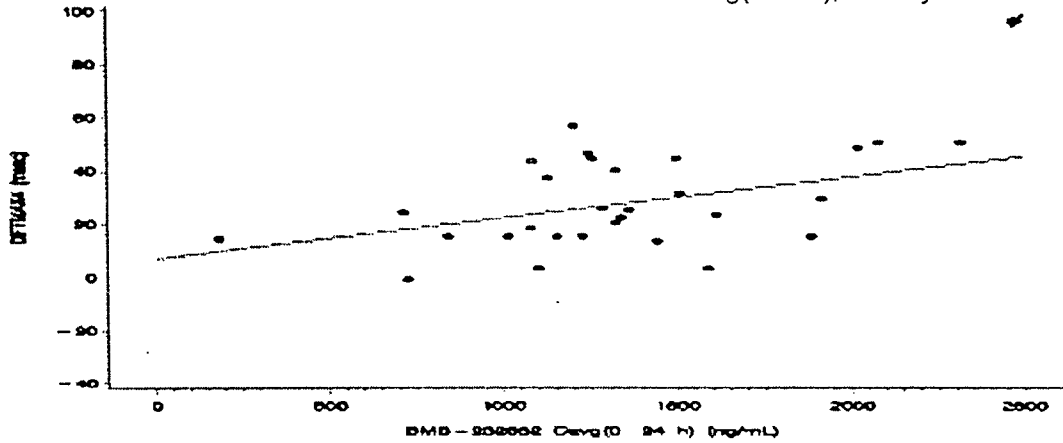
Plot of Mean PR versus Time on Days 10 and 21



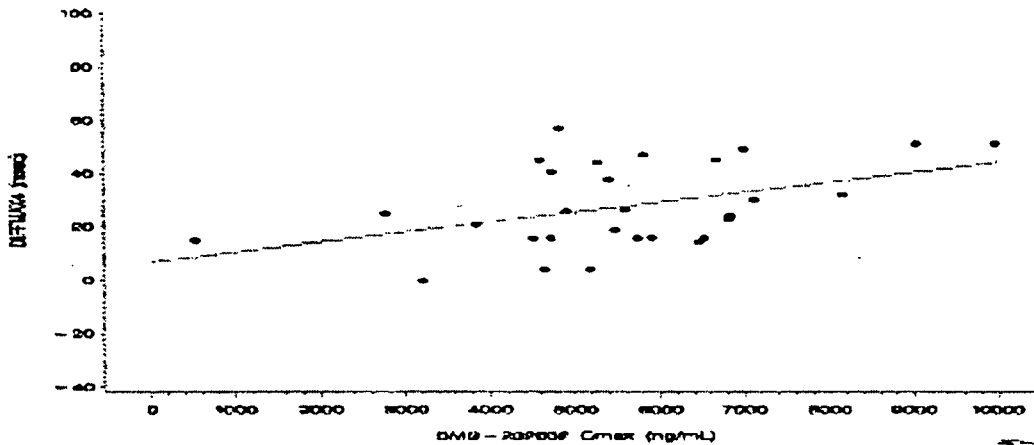
The above figures show that combination of atazanavir and clarithromycin increased PR prolongation as compared to atazanavir or clarithromycin alone. The data show that, on Day 6, six (6) subjects out of 29 (21%) had at least one derived PR measure > 200 msec, on Day 10, eleven (11) subjects out of 29 (38%) had at least one derived PR measure > 200 msec, and on Day 21, all subjects had all derived PR measures \leq 200 msec.

The following figures show that atazanavir has concentration-dependent effects on the PR interval.

Scatter Plot and Fitted Regression Line of Change from Baseline PR Max to PR Max on Atazanavir Cavg(0-24h), on Day 6



Scatter Plot and Fitted Regression Line of Change from Baseline PR Max to PR Max on Atazanavir Cmax, on Day 6



Conclusion:

- Co-administration of twice-daily doses of 500 mg of clarithromycin and once-daily doses of 400 mg of atazanavir had a small effect on the pharmacokinetics of atazanavir.
- Co-administration of twice-daily doses of 500 mg of clarithromycin and once-daily doses of 400 mg of atazanavir resulted in a 50% and 94% increase in Cmax and AUC of clarithromycin, respectively, and approximately 70% decrease in the Cmax and AUC of 14-OH clarithromycin.
- Coadministered clarithromycin and atazanavir have additive effects on the QTc interval, as compared to the effect due to administration of atazanavir or

clarithromycin alone. However, since only Bazett's correction was used, it is not known if the same effect still exists if Fridericia's correction is used.

- Atazanavir has concentration-dependent effects on the PR interval, at the 400 mg once-daily dose for 6 days in healthy subjects. The modest prolongations of the PR interval were asymptomatic and not clinically significant.
- Coadministered clarithromycin and atazanavir have additive effects on the PR interval, as compared to the effect due to administration of atazanavir alone.
- Atazanavir dose does not need to be modified when atazanavir is co-administered with clarithromycin.
- A dose reduction of clarithromycin by half (250 mg BID) is recommended when used for treatment of Mycobacterium avium complex (MAC) in patients receiving atazanavir. Consider alternative therapy for indications other than infections due to MAC.

APPEARS THIS WAY
ON ORIGINAL

APPEARS THIS WAY
ON ORIGINAL

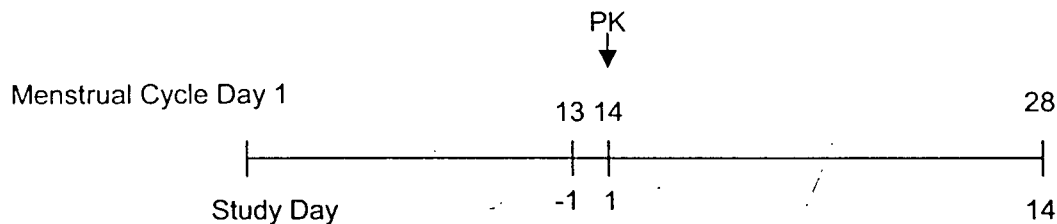
Pharmacokinetic Interaction Study of Ethinyl Estradiol and Norethindrone in Combination as Ortho-Novum 7/7/7 and BMS-232632 in Healthy Subjects (A1424030)

Objective: To assess whether atazanavir (BMS-232632) at 400 mg, administered in the presence of a light meal once-daily for 14 days, has an effect on the steady-state pharmacokinetics of either ethinyl estradiol or norethindrone.

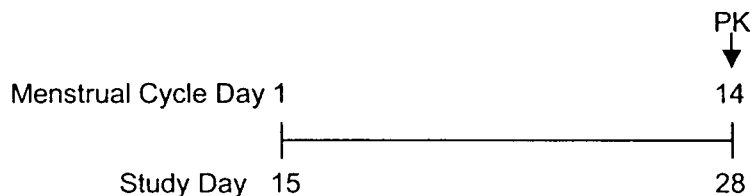
Population: 22 healthy women stabilized on an oral contraceptive regimen of Ortho-Novum® 7/7/7.

Study Design: This was an open-label, non-randomized study. Subjects entered the clinical facility on Study Day -1 after self-administration of Ortho-Novum® 7/7/7 for 13 days. They received their standard dose of Ortho-Novum® 7/7/7 on Study Day 1 and a full 24-hour pharmacokinetic profile was taken for Orth-Novum® 7/7/7. Subjects were furloughed from the clinical unit on Study Day 2 and instructed to continue daily self-administration of the remainder of their Ortho-Novum® 7/7/7 package. Subjects returned to the clinical facility the evening before the first day of the subsequent Ortho-Novum® 7/7/7 package (Study Day 15). Ortho-Novum® 7/7/7 and atazanavir at 400 mg were coadministered once-daily for 14 consecutive days. A full 24-hour pharmacokinetic profile was taken for Ortho-Novum® 7/7/7 and atazanavir on the 14th day of dosing. The drug administration is shown in the following diagram.

Menstrual Cycle 1: Ortho-Novum® 7/7/7



Menstrual Cycle 2: Ortho-Novum® 7/7/7 + atazanavir 400 mg



All doses were given within 5 minutes after a light breakfast meal.

Pharmacokinetic sampling: Blood samples were collected prior to dosing and at 0.5, 1, 1.5, 2, 2.5, 3, 4, 5, 6, 8, 10, 12, 16 and 24 h after dosing on Study Days 1 and 29.

Formulation: Atazanavir (BMS-232632-05) was supplied as 200 mg capsules (Batch # C99274). The subjects supplied the marketed drug Ortho-Novum® 7/7/7.

Analytical Analysis: Plasma samples for BMS-232632 concentrations were assayed by a validated method. Plasma samples for ethinyl estradiol and norethindrone concentrations were assayed by a validated method. The standard curve and QC data indicated that the plasma assay methods for BMS-232632, ethinyl estradiol and norethindrone were precise and accurate. See QBR for details.

Pharmacokinetic Results:

Norethindrone and ethinyl estradiol

The pharmacokinetics of norethindrone and ethinyl estradiol are presented below:

Pharmacokinetic Parameter	Day 1 ^a (n = 19)	Day 29 ^a (n = 19)
Norethindrone		
C _{max} (pg/mL) Geometric Mean (C.V. %)	11411.56 (51.71)	19056.58 (26.62)
AUC _{0-24h} (pg·h/mL) ^b Geometric Mean (C.V. %)	72904.58 (75.83)	152819.87 (31.10)
T _{max} (h) Median (Min, Max)	1.50 <u> </u>	1.50 <u> </u>
Ethinyl Estradiol		
C _{max} (pg/mL) Geometric Mean (C.V. %)	101.02 (38.62)	115.74 (28.33)
AUC _{0-24h} (pg·h/mL) ^b Geometric Mean (C.V. %)	1019.83 (42.77)	1511.56 (27.61)
T _{max} (h) Median (Min, Max)	2.00 <u> </u>	1.50 <u> </u>

^a Treatments: Day 1 = Ortho-Novum[®] 7/7/7.

Day 29 = Concomitant administration of Ortho-Novum[®] 7/7/7 and 400 mg of atazanavir.

^b TAU = 24 h

The geometric means, ratios of the geometric means, and the 95% confidence intervals for the ratios of geometric means for norethindrone and ethinyl estradiol are presented below:

Pharmacokinetic Parameter	Geometric Mean		Day 29/Day 1 Ratio Point Estimate (95% C.I.)
	Day 1 ^a	Day 29 ^a	
Norethindrone			
C _{max} (pg/mL)	11411.56	19056.58	1.67 (1.42, 1.96)
AUC (TAU) (pg·h/mL) ^b	72904.58	152819.87	2.10 (1.68, 2.62)
Ethinyl Estradiol			
C _{max} (pg/mL)	101.02	115.74	1.15 (0.99, 1.32)
AUC (TAU) (pg·h/mL) ^b	1019.83	1511.56	1.48 (1.31, 1.68)

^a Treatments Day 1 = Ortho-Novum[®] 7/7/7.

Day 29 = Coadministration of Ortho-Novum[®] 7/7/7 and 400 mg of atazanavir.

^b TAU = 24h

The data show that atazanavir increased norethindrone and ethinyl estradiol plasma concentrations. Ethinyl estradiol and norethindrone are two commonly used oral contraceptive hormones. Following oral administration, both ethinyl estradiol and norethindrone undergo first pass metabolism. Oxidation by CYP3A and conjugation by glucuronidation (the principal uridine diphosphate-glucuronosyl transferase (UGT) isoform is 1A1) and sulfation are the pathways responsible for the metabolism of ethinyl estradiol. The enzymes responsible for and their relative contribution to the metabolism of norethindrone have not been well characterized, although hydroxylated, sulfated, and glucuronidated metabolites of norethindrone have been detected. Atazanavir is an inhibitor of the CYP3A4 isozyme and UGT1A1, and thus it could increase norethindrone and ethinyl estradiol plasma concentrations.

Marketed oral contraceptives generally contain 20 µg to 50 µg ethinyl estradiol. Since, a roughly proportional dose-exposure relationship for ethinyl estradiol exists in the range of 35 to 50 micrograms, the exposure produced by coadministration of 35 micrograms of ethinyl estradiol with atazanavir is closer to that produced by 50 micrograms of ethinyl estradiol. Cardiovascular risks, specifically thrombosis, are the most common risks associated with ethinyl estradiol administration.

Progestins have been associated with impairment of lipid and glucose metabolism. However, there are no formal dose-response data for these parameters. As the change in these parameters at risk is not quantified, for these parameters, caution is warranted.

The applicant recommended the lowest effective dose of each oral contraceptive component be used, which is acceptable.

Atazanavir

The pharmacokinetics of atazanavir are presented below:

Pharmacokinetic Parameter	Day 29 ^a (n = 18)
C _{max} (ng/mL) Geometric Mean (C.V. %)	4369.74 (26.07)
AUC(TAU) (ng·h/mL) ^b Geometric Mean (C.V. %)	22856.85 (35.42)
T _{max} (h) Median (Min, Max)	2.25
T-1/2 ^c Mean (S.D.)	8.72 (2.78)

^a Treatments Day 29 - Coadministration of Ortho-Novum[®] 7/7/7 and 400 mg of atazanavir.

^b TAU = 24 h

^c n = 17

The pharmacokinetic parameters of atazanavir in this study were similar to those observed previously in healthy subjects at steady-state, suggesting a lack of influence of Ortho-Novum[®] 7/7/7 on the pharmacokinetics of atazanavir.

The rates of hyperbilirubinemia in this study were similar to those observed in other studies where 400 mg atazanavir was administered. The conversion of unconjugated bilirubin was seemingly unaffected by the presence of ethinyl estradiol.

Conclusion:

- Coadministration of once-daily doses of Ortho-Novum[®] 7/7/7 and atazanavir at 400 mg resulted in a 67% and 110% increase in the C_{max} and AUC of norethindrone, respectively, compared to the administration of Ortho-Novum[®] 7/7/7 alone.
- Coadministration of once-daily doses of Ortho-Novum[®] 7/7/7 and atazanavir at 400 mg resulted in a 15% and 48% increase in the C_{max} and AUC of ethinyl estradiol, respectively, compared to the administration of Ortho-Novum[®] 7/7/7 alone.
- The lowest effective dose of each oral contraceptive component is recommended.

Randomized, Double-Blind, Placebo Controlled, Multiple-Dose Three-Way
Crossover Study of the Electrocardiographic Effects of Atazanavir in Healthy Adult
Subjects (A1424076)

Objective: To determine the effect of atazanavir on the QTc and PR intervals. To assess the multiple-dose pharmacokinetics of atazanavir at the 400 and 800 mg dose levels, when administered with a light meal.

Population: A total of 72 subjects, age ranged from 19 to 50 years (mean = 30 years), were enrolled in this study. Sixty-four (64) subjects (47 males, 17 females) completed the study.

Study Design: This was a double-blind, randomized, placebo-controlled, multiple-dose, three-period, three-treatment crossover study, balanced for residual effects, in healthy subjects. Each subject received the following three treatments (A, B, C) for 6 days with a washout period of at least 14 days between treatments, in one of six randomly assigned treatment sequences.

A: 4 x 200 mg matching placebo capsules QD.

B: 2 x 200 mg atazanavir capsules and 2 x 200 mg matched placebo capsules QD.

C: 4 x 200 mg atazanavir capsules QD.

All doses were given within 5 minutes after each subject consumed a light meal.

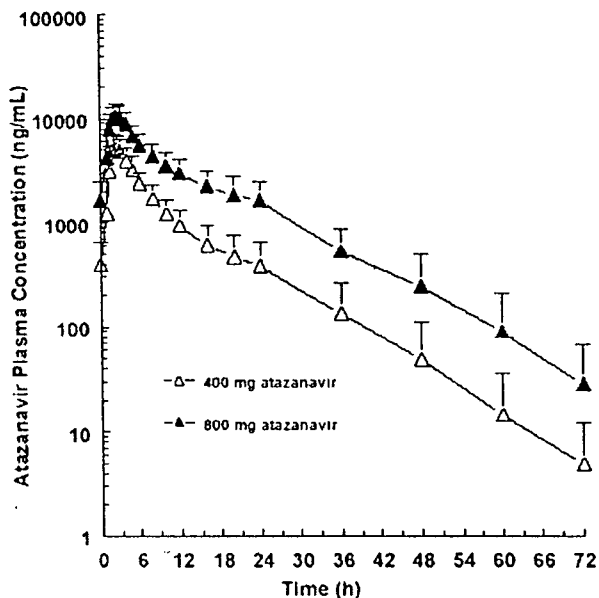
Formulation: BMS-232632 200-mg capsules (Batch # N00024).

Pharmacokinetic Sampling: PK blood samples were collected at pre-dose and 1, 1.5, 2, 2.5, 3, 4, 5, 6, 8, 10, 12, 16, 20 and 24 hours after dosing on Day 6 of each treatment period and at pre-dose on Days 2 and 4 of each treatment period. In addition, PK blood samples were collected at 36, 48, 60 and 72 hours after dosing on Day 6 of Period 1 only.

Twelve (12)-lead ECGs were recorded at screening; on Day -1 and on Day 6 (at the same clock times as the ECGs recorded on Day -1) at pre-dose and at 1, 2, 2.5, 3, 4, 6, 8, 12, 16, 20 and 24 hours after dosing, on each treatment period.

Analytical Analysis: Plasma samples were assayed for BMS-232632 concentrations by validated methods. The standard curve and QC data indicated that the plasma assay methods for BMS-232632 were acceptable. See QBR for details.

Pharmacokinetic Results: The mean plasma concentration-time profiles and the mean pharmacokinetic parameters of BMS-232632 following administration of 400 mg and 800 mg QD regimens are shown in the following figure and table.



Pharmacokinetic Parameter	Treatment	
	ATV at 400 mg (n = 65)	ATV at 800 mg (n = 66) ^a
C _{max} (ng/mL) Geometric Mean (C.V.%)	5500 (34)	11102 (27)
AUC ₍₀₋₂₄₎ (ng·h/mL) ^b Geometric Mean (C.V.%)	33097 (36)	90432 (29)
T _{max} (h) Median (Min. Max)	2.50 (—)	2.50 (—)

^a Data from Subject AI424076-1-29 were excluded.

^b AUC = 24 h

Note: Subject AI424076-1-29 vomited three times at 0:20, 0:47, and 1:52 hours post-dosing on Day 3 of Period 2.

Compared to Study AI424040, the C_{max} and AUC of atazanavir in this study are 30% and 41% higher, respectively, at the 400 mg dose; and are 15% and 25% higher at the 800 mg dose. However, the C_{max} and AUC at the 400 mg dose are comparable to values observed in Studies AI424057 and AI424055. The data suggest that the exposure to atazanavir (AUC) increased in a proportion greater than the dose. The time to reach C_{max} was similar for both treatments, and comparable to other studies.

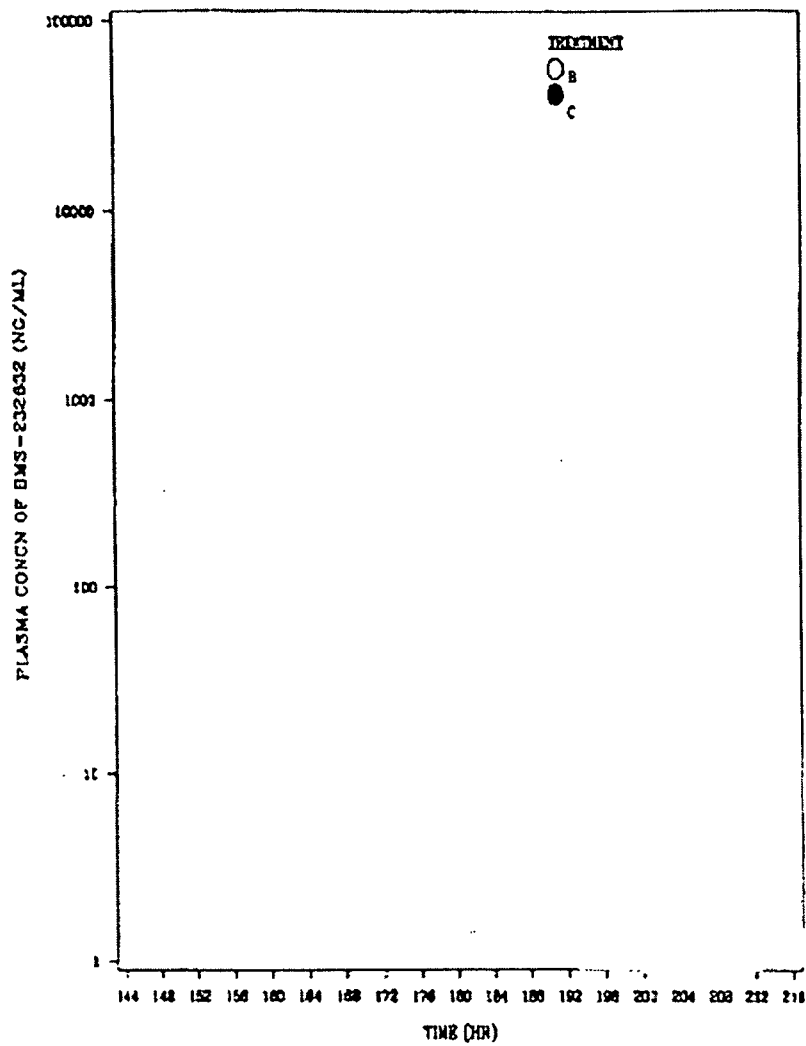
As the subjects were sampled for 72 hours in Period 1 and for 24 hours in Periods 2 and 3, T_{1/2} values have been summarized separately by treatment period in the following table.

T-HALF (h)	Treatment	
	ATV at 400 mg	ATV at 800 mg
Period 1 n Mean (S.D.)	24 6.27 (1.41)	23 7.25 (1.99)
Period 2 n Mean (S.D.)	20 10.21 (6.22)	22 30.39 (57.93)
Period 3 n Mean (S.D.)	21 11.77 (5.40)	21 ^a 24.49 (22.63)

^a Data from Subject AI424076-1-29 was excluded.

The mean T-HALF values observed with 72 h of sampling in Period 1 were 6.27 h and 7.25 h following 400 mg and 800 mg doses of atazanavir, respectively. These values are consistent with a previous study (AI424040) where the mean T-HALF values were 7.06 h and 9.91 h following 400 mg and 800 mg QD doses of atazanavir for 5 days, respectively. However, the mean T-HALF values following 24 hours of sampling in Periods 2 and 3 of this study were somewhat longer and were approximately 10 h and 25 h at 400 mg and 800 mg doses of atazanavir, respectively. At the dose of 800 mg, sampling for 24 h resulted in T-HALF values for five subjects ranging from 54 to 282 h. The relatively prolonged T-HALF values observed in the current study with 24 h of sampling are likely due to enterohepatic recycling close to the end of the sampling as shown in the following figure. The pattern of flatter decrease of plasma concentration near 24 hour after dosing was seen in every subject in the study. The exposures obtained with the 800 mg dose (C_{max} = 11102 ng/mL, AUC = 90432 ng. h/mL) were higher than those seen with the once-daily doses of 300/100 mg atazanavir/ritonavir regimen (C_{max} = 6129 ng/mL, AUC = 57039 ng. h/mL).

APPEARS THIS WAY
ON ORIGINAL



The following table summarizes statistics for atazanavir plasma trough concentrations. Trough concentrations suggest that steady-state was achieved within six days of once daily doses of 400 mg and 800 mg atazanavir.

C _{min} (ng/mL)	Treatment	
	ATV at 400 mg (n = 65) ^a	ATV at 800 mg (n = 68) ^b
Day 2 Mean (S.D.)	92 (70)	525 (310)
Day 4 Mean (S.D.)	337 (210)	1350 (730)
Day 6 Mean (S.D.)	385 (260)	1624 (832) ^c
Day 7 Mean (S.D.)	378 (271)	1642 (856) ^d

AI424076

Source: Supplemental Table S 11.2.1E

^a n = 64 for Day 2

^b n = 67 for Day 6, n = 66 for Day 7

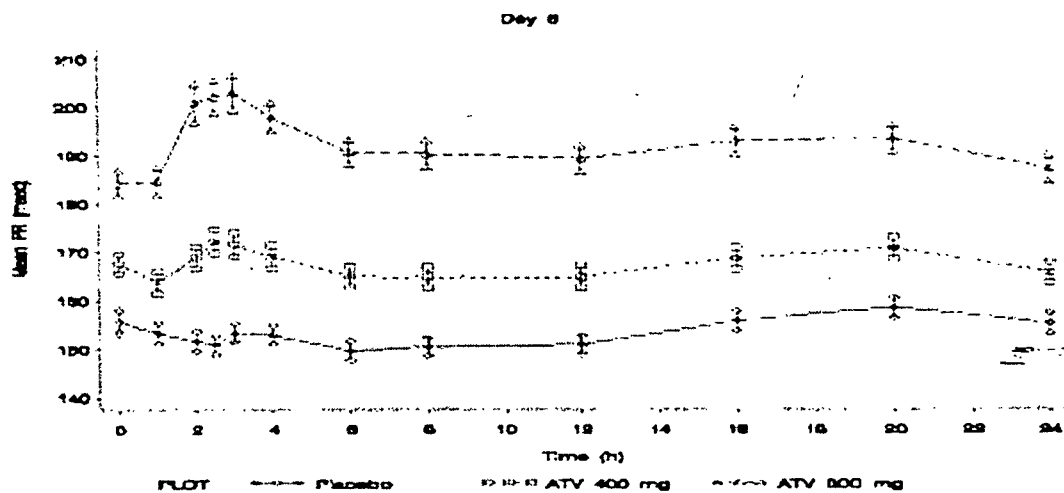
^c Data from Subject AI424076-1-17 was excluded

^d Data from Subject AI424076-1-29 was excluded

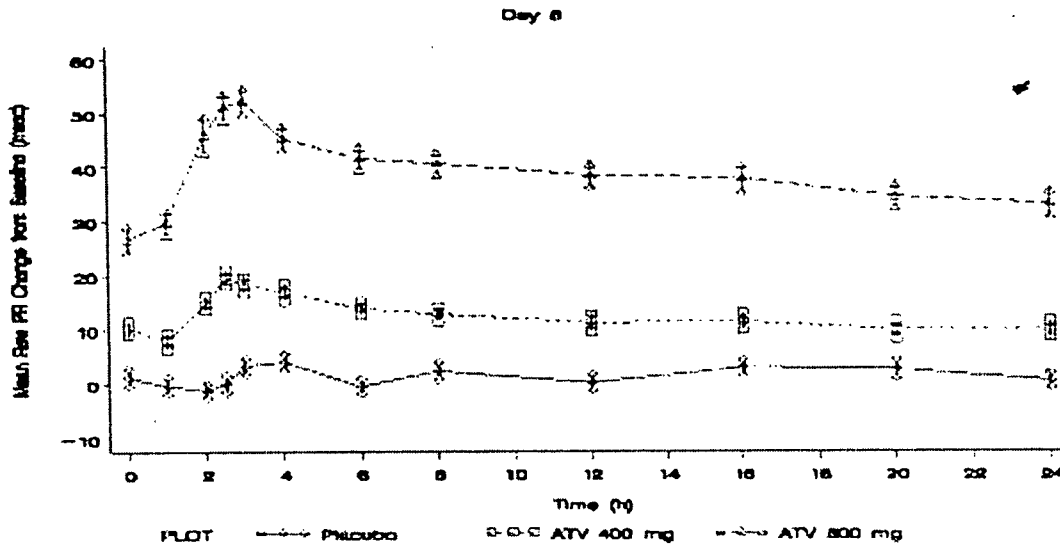
Note: For Subject AI424076-1-17, a pre-dose sample was taken on Day 6 of Period 1, even though the subject had received the last dose of study drug on Day 4 of Period 1.

PR interval

Plot of Mean PR (± SE) Versus Time Since Dosing on Day 6

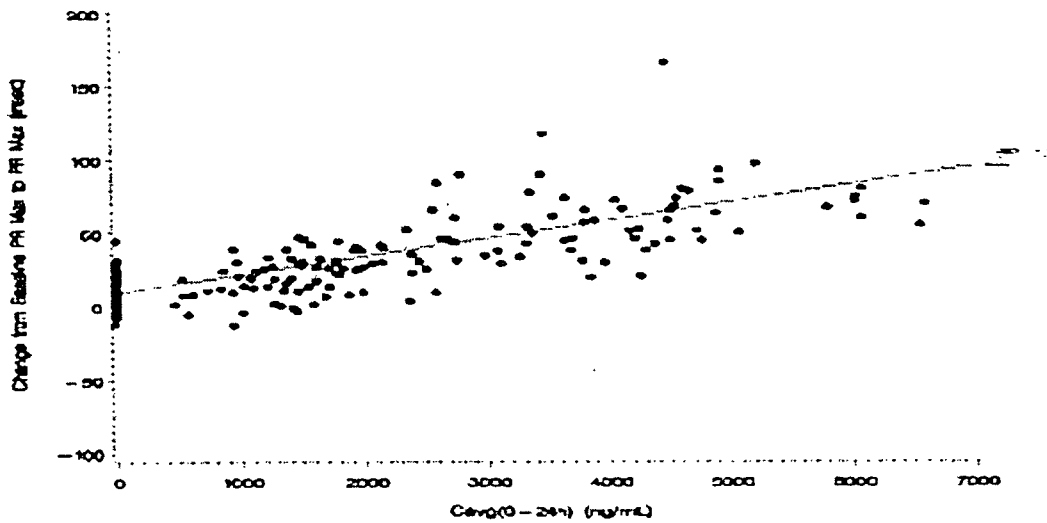


Plot of Mean Raw PR Change (\pm SE) from Baseline versus Time Point on Day 6

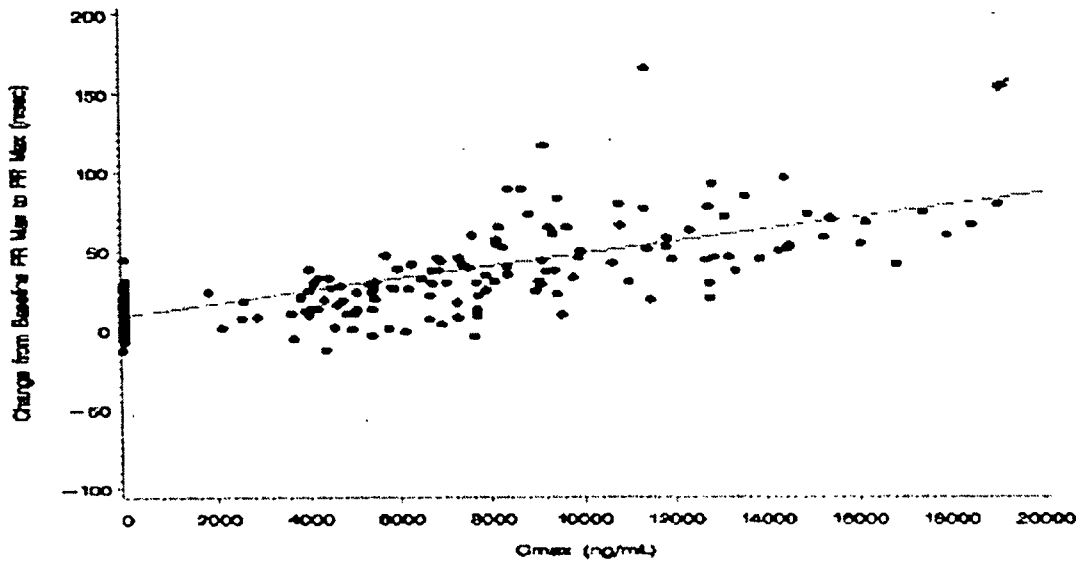


These plots suggest a clear dose-response effect of atazanavir on the PR interval, with the peak effect at approximately the time of peak plasma concentration (median T_{max} = 2.5 h).

Scatter Plot and Fitted Regression Line of Change from Baseline PR Max to PR Max on Atazanavir C_{avg} (0-24h)



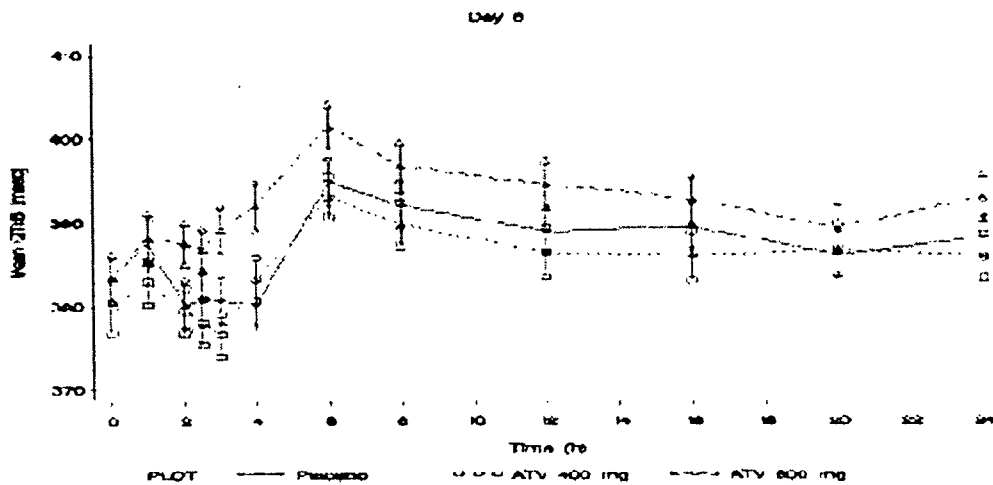
Scatter Plot and Fitted Regression Line of Change from Baseline PR Max to PR Max on Atazanavir Cmax



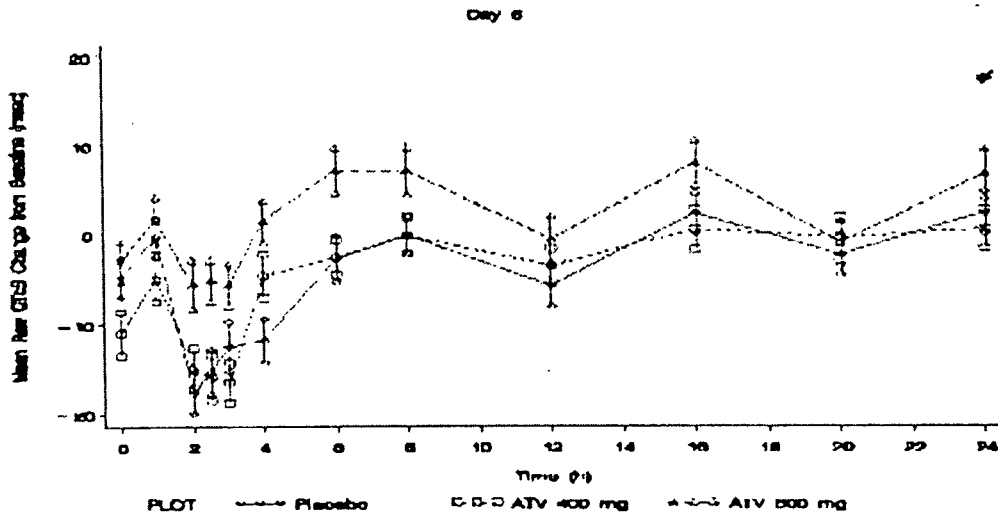
The data showed that there was a statistically significant concentration-dependent effect of atazanavir on the PR interval. The frequency of PR prolongations (> 200 msec) was dose-dependent (59% for ATV at 800 mg, 14 % for ATV at 400 mg, 1% for placebo). The observed PR prolongations were generally mild and reversible, asymptomatic, and not associated with 2nd or 3rd degree AV block.

QTc interval

Plot of Mean QTcB (\pm SE) Versus Time since Dosing on Day 6

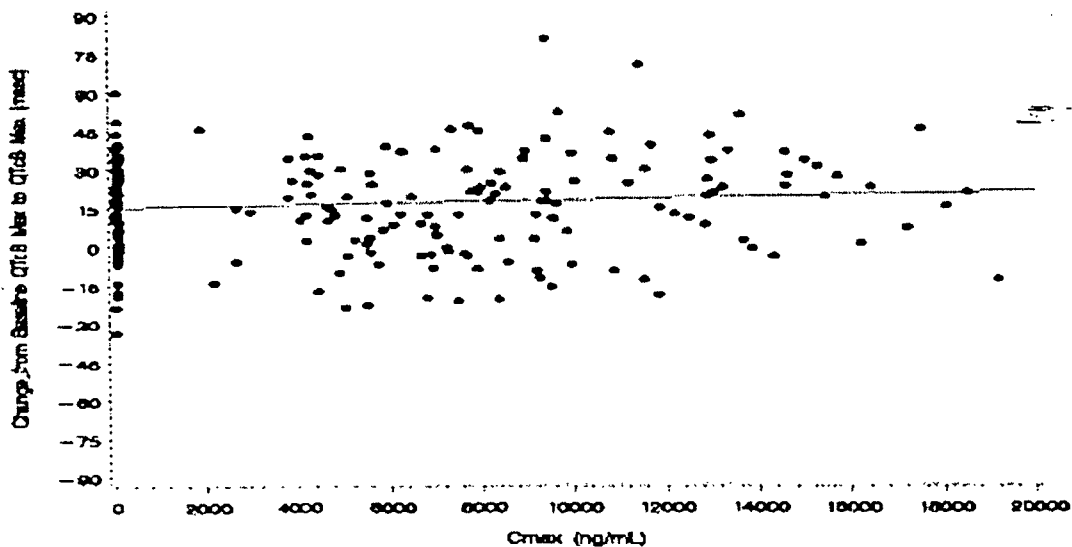


Plot of Mean Raw QTcB Change from Baseline versus Time Since Dosing on Day 6

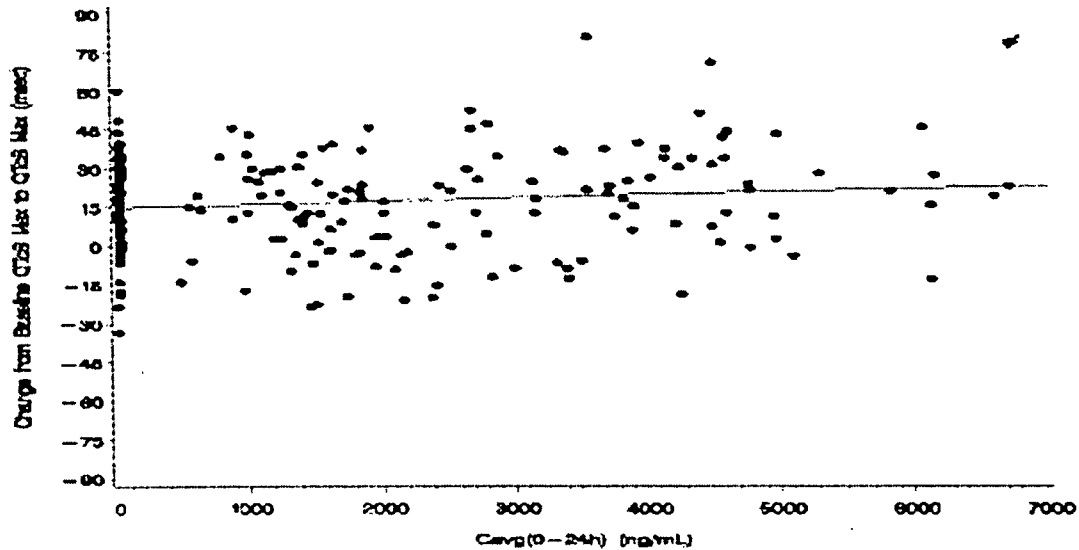


This plot suggests that atazanavir at 400 mg does not have an effect on the QTcB interval as compared to the effect of placebo. The mean QTcB change from baseline for atazanavir at 800 mg tended to be larger than that for placebo and for atazanavir at 400 mg, over the 24 hours. The placebo-corrected, time-matched mean change from baseline to QTcB at Tmax (Δ_1 QTcB at Tmax) was -3.4 msec for the 400 mg dose and +7.9 msec for the 800 mg dose of atazanavir. The placebo-corrected (difference between the adjusted mean for atazanavir and the adjusted mean for placebo), mean time-matched change from baseline to QTcB Max (Δ_1 QTcB Max) was -5.1 msec for the 400 mg dose and +1.2 msec for the 800 mg dose of atazanavir.

Scatter Plot and Fitted Regression Line of Change from Baseline QTcB Max to QTcB Max on Atazanavir Cmax



Scatter Plot and Fitted Regression Line of Change from Baseline QTcB Max to QTcB Max on Atazanavir Cavg (0-24h)



The above plots show that QTcB prolongation tends to be increased with increased atazanavir concentrations. The applicant did linear regression analysis and indicated that there was not a statistically significant increase with increased concentrations. However, since there may be a significant lag time between the occurrence of maximum QTcB prolongation and maximum plasma concentrations, this method may not be useful especially by using maximum QTcB. The 95% confidence interval for the population slope of the linear regression of change from baseline QTcB Avg to QTcB Avg on atazanavir Cavg(0-24h) was above zero, as shown in the following table. Using QTcB Avg may be more sensitive when there is a delay effect.

APPEARS THIS WAY
ON ORIGINAL

Δ QTcB ^a (msec)	C _{avg} (0-24h) (ng/mL)				
	Intercept			Slope	
	n ^b	Point Estimate	95% C.I.	Point Estimate	95% C.I.
Δ_1 QTcB Max	199	15.21	(11.49, 18.92)	0.0013	(-0.0004, 0.0029)
Δ_2 QTcB Max	199	17.33	(14.61, 20.06)	0.0007	(-0.0006, 0.0020)
Δ_3 QTcB Max	199	20.62	(17.40, 23.84)	0.0006	(-0.0008, 0.0020)
Δ_1 QTcB at T _{max}	199	-16.36	(-20.35, -12.37)	0.0025	(0.0009, 0.0042)
Δ_2 QTcB at T _{max}	199	-11.32	(-14.59, -8.05)	0.0018	(0.0005, 0.0031)
Δ_3 QTcB at T _{max}	199	-7.86	(-11.69, -4.04)	0.0016	(-0.0000, 0.0031)
Δ_1 QTcB Avg	199	-4.13	(-6.15, -2.12)	0.0018	(0.0009, 0.0028)
Δ_2 QTcB Avg	199	-0.83	(-3.47, 1.81)	0.0017	(0.0005, 0.0028)

A1424076

Source: Appendix 12.8.2.1G

^a QTcB Changes from Baseline

Δ_1 QTcB Max = Change from baseline QTcB Max to QTcB Max

Δ_2 QTcB Max = Change from baseline QTcB Avg to QTcB Max

Δ_3 QTcB Max = Change from QTcB at Pre-dose to QTcB Max

Δ_1 QTcB at T_{max} = Change from baseline QTcB at T_{max} to QTcB at T_{max}

Δ_2 QTcB at T_{max} = Change from baseline QTcB Avg to QTcB at T_{max}

Δ_3 QTcB at T_{max} = Change from baseline QTcB at Pre-dose to QTcB at T_{max}

Δ_1 QTcB Avg = Change from baseline QTcB Avg to QTcB Avg

Δ_2 QTcB Avg = Change from baseline QTcB at Pre-dose to QTcB Avg

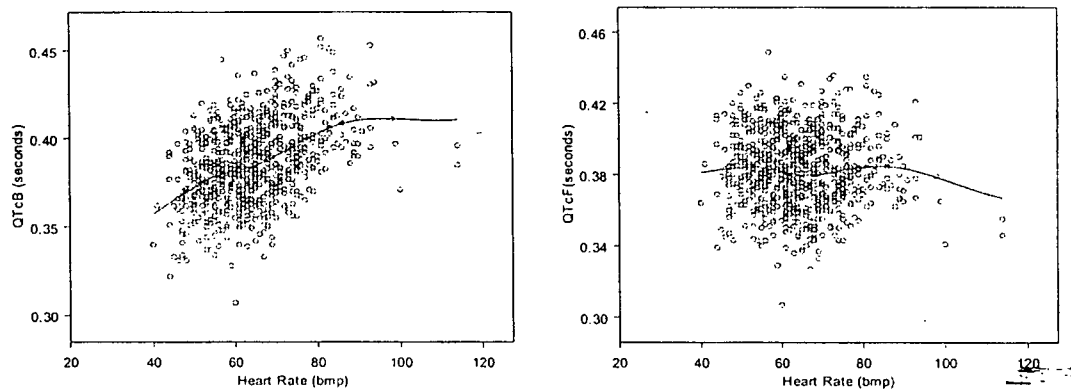
^b n is the number of data pairs in the analyses (64 subjects had data from 3 periods, 1 subject had data from 2 periods, and 5 subjects had data from one period)

The frequency of subjects with prolonged QTcB (> 450 msec for males, > 470 msec for females) was similar at baseline, for placebo and for the 400 mg and 800 mg doses of atazanavir as shown in the following table.

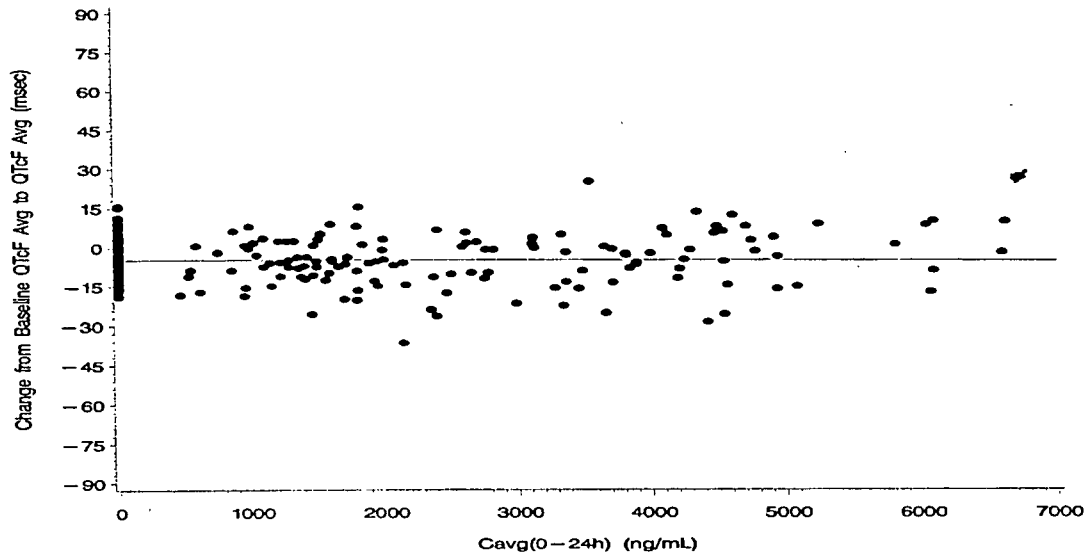
Treatment	QTcB Interval (msec)					
	Male n (%)			Female n (%)		
	431-450	>450	>500	451-470	>470	>500
Prior to Dosing (n=72, 54M, 18F)	9 (17%)	2 (4%)	0 (0%)	2 (11%)	1 (6%)	0 (0%)
Placebo (n=67, 50M, 17F)	5 (10%)	0 (0%)	0 (0%)	2 (12%)	0 (0%)	0 (0%)
ATV 400 mg (n=65, 48M, 17F)	2 (4%)	0 (0%)	0 (0%)	0 (0%)	0 (0%)	0 (0%)
ATV 800 mg (n=66, 50M, 16F ^a)	4 (8%)	1 (2%)	0 (0%)	2 (13%)	1 (6%)	0 (0%)
All ATV Doses (n=67, 50M, 17F)	4 (8%)	1 (2%)	0 (0%)	2 (12%)	1 (6%)	0 (0%)

The frequency of subjects with prolonged $\bar{Q}TcB$ (> 60 msec) was similar for placebo ($n = 1$) and for the 400 mg dose ($n = 0$) of atazanavir, and it was slightly greater for the 800 mg dose of atazanavir ($n = 3$).

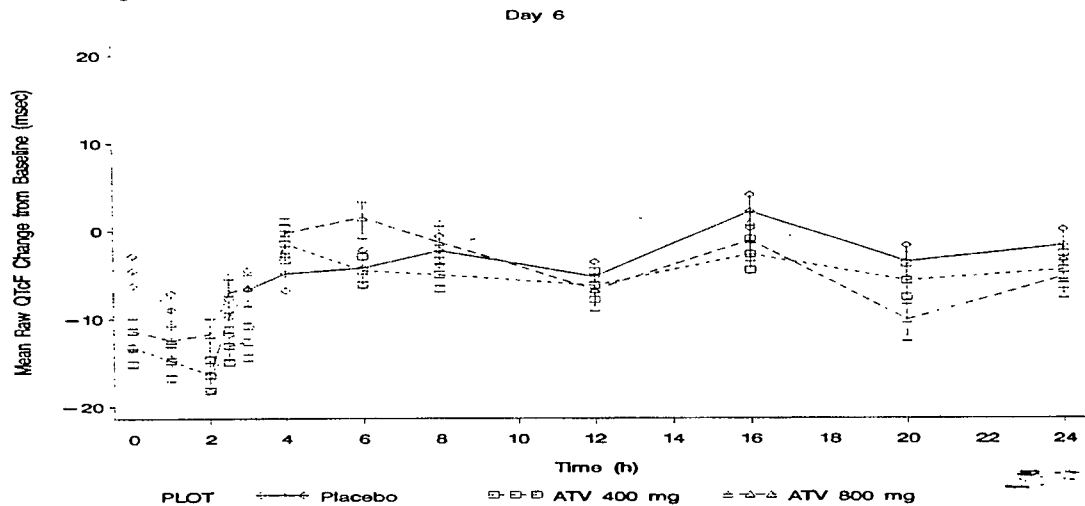
The sponsor used Bazett's correction ($QTcB$). My analysis with placebo subjects shows that $QTcB$ increased with increased heart rates, while Fridericia's corrected QT ($QTcF$) is constant with increase heart rates except at very extreme heart rates, where $QTcF$ is underestimated, as shown in the following figures (solid lines are loess fit).



We asked the applicant to reanalyze QT by Fridericia's formula during the review. The reanalysis showed that no subject had any ECG with prolonged $QTcF$ (>450 msec for males, > 470 msec for females) or with prolonged $QTcF$ change from baseline (> 60 msec). The following figure showed that for each additional 1000 ng/mL of $C_{avg}(0-24h)$, the estimated $QTcF$ changes from baseline ranged between -0.8 and 0.5 msec. All 95% confidence intervals for the slopes for the linear regressions of $QTcF$ changes from baseline on $C_{avg}(0-24h)$ included zero. All upper bounds of the 95% confidence intervals for the slopes were below 6 msec per 1000 ng/mL, the largest being 1.8 msec per 1000 ng/mL.

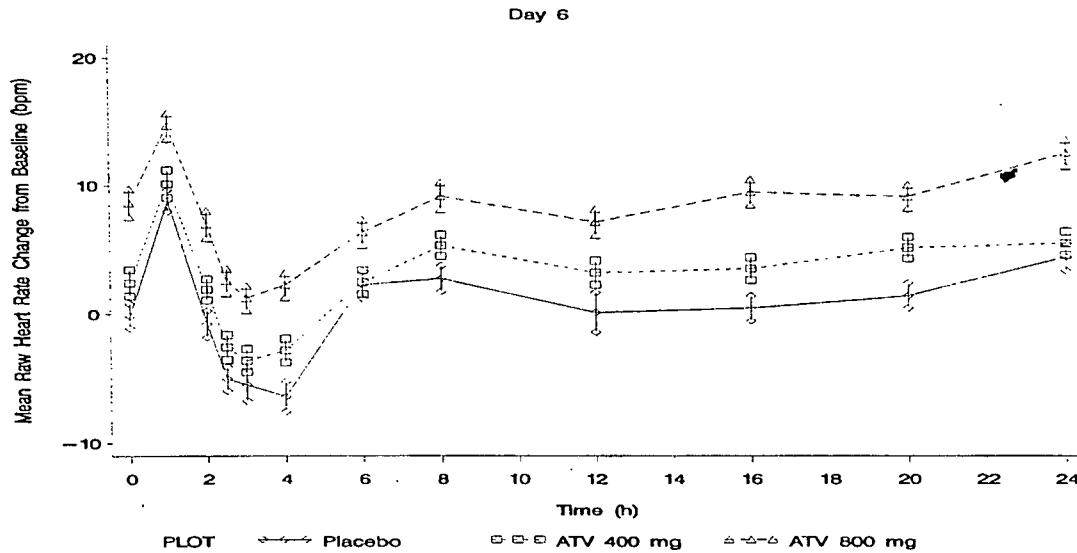


Placebo-corrected (difference between the adjusted means for ATV and for placebo) mean Δ_1 QTcF Max was -6.1 msec for the 400 mg dose and -3.4 msec for the 800 mg dose of ATV, as shown in the following figure.



Note: Vertical bars represent one S.E. of the mean.

A plot of mean raw (time-matched) heart rate changes from baseline versus time since dosing on Day 6 is presented in the following figure.



Atazanavir appears to be associated with a modest dose-dependent increase in heart rate compared to placebo. Compared to the placebo, heart rate increased 3.5 beats/min at the 400 mg dose, and 8.2 beats/min at the 800 mg dose. In this setting, Fridericia's formula may be more appropriate than Bazett's formula for heart rate correction of QT.

Conclusion:

- Multiple once-daily dosing produced a greater than dose proportional increase in the exposure of atazanavir. An increase in the dose of 1:2 produced an increase of 1:2.7 in the atazanavir exposure.
- Atazanavir was rapidly absorbed with a median T_{max} of 2.5 hours following 400 mg and 800 mg QD doses for 6 days. Steady-state appeared to have been achieved within 6 days, with mean T_{1/2} values of 6 - 7 h for both atazanavir doses.
- The frequency of subjects with prolonged QTcB (> 60 msec) was similar for placebo (n = 1) and for the 400 mg dose (n = 0) of atazanavir, and it was slightly greater for the 800 mg dose of atazanavir (n = 3).
- No subject had any prolonged QTcF (> 450 msec for male, > 470 msec for females) or prolonged ΔQTcF (> 60 msec).
- Atazanavir is associated with a modest dose-dependent increase in heart rate compared to placebo. In this setting, Fridericia's formula may be more appropriate than Bazett's formula for heart rate correction of QT.
- Atazanavir has a statistically significant concentration-dependent effect on the PR interval.
- PR prolongations (PR > 200 msec) were dose-related and their frequency and magnitude increased with increasing dose of atazanavir. No episodes of 2° or 3° AV-block were observed at all dose levels.

Background: The applicant developed a population pharmacokinetic structural model for atazanavir using Phase I data collected from Protocols AI424002 and AI424040 (Report 930002915). To help the dose selection for Phase III trials, the applicant also performed an interim analysis of data collected from patients enrolled in protocol AI424007 (Report AI424007). Since this analysis was interim and the patients' food status at the time of the dose was unknown, the Phase I model available for the interim analysis was developed using fasted data. The analysis was limited to only the data collected during the two-week monotherapy phase at the beginning of the trial. An analysis (Report 930002847) was conducted to characterize the full final pharmacokinetic and antiviral activity of the Phase II data collected in studies AI424007 and AI424008 combined. In this analysis, only patients dosed under fed condition were included. This review focuses on the last PK/PD analysis.

Objectives: The Phase I model (Report 930002915) was developed to establish structural model for Phase II population PK analysis. The interim analysis of data collected from patients enrolled in protocol AI424007 (Report AI424007) was used to help the dose selection for Phase III trials. The population pharmacokinetic/pharmacodynamic analysis based upon data collected from HIV-positive subjects in two Phase II studies, AI424007 and AI424008 (Report 930002847), had three objectives:

1. To develop a Phase II pharmacostatistical model incorporating the appropriate structural PK model, as well as any relationships between key pharmacokinetic parameters and selected subject covariates using the data collected from subjects enrolled in both Protocols AI424007 and AI424008;
2. To develop an exposure-antiviral activity model for Protocols AI424007 and AI424008 evaluating activity at selected timepoints throughout the study, as well as explore any influential covariate relationships;
3. To develop an exposure-safety model for Protocols AI424007 and AI424008 evaluating total bilirubin at selected timepoints, as well as to explore any influential covariate relationships.

Impact of the Population PK/PD Analysis: The only population PK/PD analysis results used in the Package Insert is the effect of race on the PK of atazanavir. An interim analysis of data collected from patients enrolled in protocol AI424007 (Report AI424007) was used to help the dose selection for Phase III trials.

Study Design:

Phase I

1. *AI424002: A randomized, double-blind, placebo-controlled, multiple-dose, dose escalation study to evaluate the safety and pharmacokinetics of BMS-232632 in healthy subjects.*

Seven cohorts (200 mg QD, 400 mg QD, 600 mg QD, 500 mg QD, 200 mg BID, 100 mg BID, and 800 mg QD for 14 consecutive days) were studied. One cohort (600 mg QD) was initially halted (after 8-day dosing) due to a protocol specific stopping rule and a second 600 mg cohort was dosed (before 800 mg QD dose) successfully. Atazanavir was administered under fasted conditions.

2. *AI424040: Open-label, randomized, three-way crossover study to evaluate the pharmacokinetics and safety of BMS-232632 administered with a light meal in healthy subjects*

This was an open-label, randomized, three-period, three-treatment, crossover study balanced for residuals. Subjects were randomized to receive three treatments (200 mg, 400 mg, and 800 mg QD x 5 days), with no washout period, in one of six randomly assigned treatment sequences. All doses were given within 5 minutes after a light meal.

3. *AI424007: Evaluation of the safety and antiviral efficacy of a novel HIV-1 protease inhibitor, BMS-232632, alone and in combination with d4T and ddI as compared to a reference combination regimen*

This was a two-stage, randomized, active-controlled, four-arm study designed to evaluate and compare the safety, tolerability, and antiviral activity of atazanavir. This study was blinded and placebo controlled with respect to atazanavir dose levels only. The first two weeks of each treatment arm were composed of atazanavir (200 mg, 400 mg or 500 mg) or nelfinavir (NFV) monotherapy followed by an additional 46 weeks of combination therapy (+ ddI +d4T). The protocol was originally indicated to give atazanavir under fasted conditions, and amended during the clinical trial to state that atazanavir should be taken once daily with a meal or snack and at least one hour apart from ddI. This resulted in a final dataset that is a composite of both fed and fasted administration.

AI424008: Evaluation of the safety and antiviral efficacy of a novel HIV-1 protease inhibitor, BMS-232632, alone and in combination with d4T and 3TC as compared to a reference combination regimen

This was a randomized, active-controlled, three-arm study designed to evaluate and compare the safety, tolerability, and antiviral activity of atazanavir at two different dose levels (400 and 600 mg QD), administered with light meal, to NFV, all in combination with d4T and 3TC over 48 weeks. This study was blinded and placebo controlled with respect to atazanavir dose levels only and did not have a two-week monotherapy phase.

Data Used for Final Population PK Analysis:

Pharmacokinetic Analysis:

Phase II data:

The bioavailability of atazanavir increased by 57% -70% when atazanavir was administered with light meal. Thus, when evaluating the data collected in Phase II, assignment of the appropriate classification of fed or fasted dose administration was important. However, the date/time of the last meal was surveyed during PK sampling visits. The applicant indicated this response could represent a meal close to the time of sampling instead of a meal close to the time of dosing. Preliminary investigations yielded an approximate mean/median difference in time between the meal and the dose of 14.8/8 hours, respectively. The applicant indicated no definite conclusion regarding the meal status at the time of dose administration could be made. Approximately half of the

data from AI424007 and a quarter of the data from AI424008 were affected by this data collection error.

The Phase I pharmacokinetic model for data associated with both fed and fasted administration incorporated not only an influence of food on bioavailability but also enterohepatic recycling. However, the data necessary to accurately model the influence of enterohepatic recycling was also not collected.

Given that the targeted dose administration instructions indicate that atazanavir should be administered with food, the applicant decided to simplify the pharmacokinetic model to a model evaluating data associated with fed administration only.

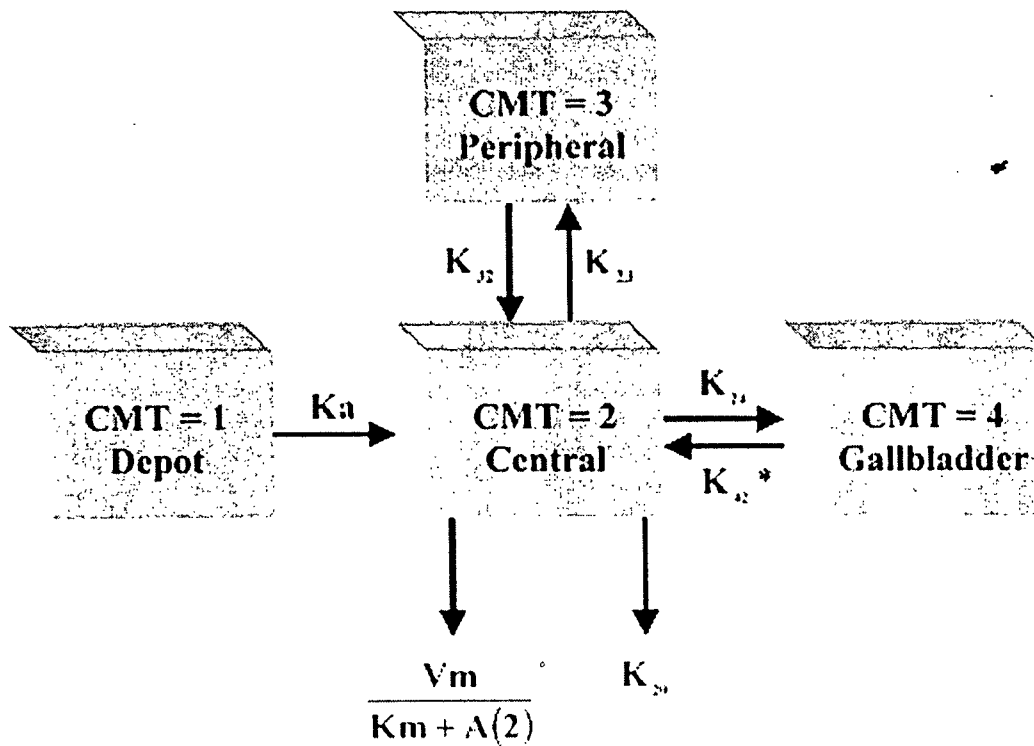
Plasma samples for population pharmacokinetic evaluations were collected at Weeks 2, 4, 12, 24, and 48. All visit draws were to occur at least 3 hours after the prior dose. A total of 195 concentrations (46%) collected from 121 subjects enrolled in Protocol AI424007 were used for the pharmacokinetic analysis. A total of 999 concentrations (50%) from 290 subjects enrolled in Protocol AI424008 were available for the pharmacokinetic analysis.

Final Pharmacokinetic Analysis Methodology:

Phase I

Several models have been evaluated. The most robust model that could be fit to the Phase I population data base (final model) was a two-compartment model with first-order absorption, first-order plus Michaelis-Menten elimination, and enterohepatic recycling. The model is a collapsed enterohepatic recycling model, because NONMEM was unable to successfully minimize in the estimation of a model in which the gall bladder would empty to the depot compartment and subsequently be reabsorbed from the depot back to the central compartment. The graphical representation of this model is shown in the following figure.

**APPEARS THIS WAY
ON ORIGINAL**



Differential Equations:

$$DADT(1) = -K_a \cdot A(1)$$

$$DADT(2) = K_a \cdot A(1) + K_{12} \cdot A(3) + K_{42} \cdot A(4) - \left(\frac{V_m}{K_m + A(2)} + K_{21} + K_{20} + K_{14} \right) \cdot A(2)$$

$$DADT(3) = -K_{12} \cdot A(3) + K_{21} \cdot A(2)$$

$$DADT(4) = -K_{14} \cdot A(4) + K_{42} \cdot A(4)$$

$$\text{Total Clearance (L/hr)} = K_{20} \cdot V_c + \left(\frac{V_m}{\left(\frac{K_m}{V_c} \right) + C_{ss}} \right)$$

*Due to the sampling strategy employed in these phase I clinical trials, the flow of drug from the gallbladder to the depot compartment and the re-absorption of drug back to the central compartment was collapsed and modeled as the flow of drug directly back to the central compartment. Thus, the rate constant, K_{42} , represents the return of drug from the gallbladder to the central compartment and serves as a composite of the complete enterohepatic recycling process.

A log residual error model was employed in the final model.

Phase II

The two-compartment model with Michaelis-Menten plus linear elimination and a log_e residual error model, was used for Bayesian prediction of the concentrations collected in these Phase II clinical trials. The PK parameters and inter- and intraindividual variability

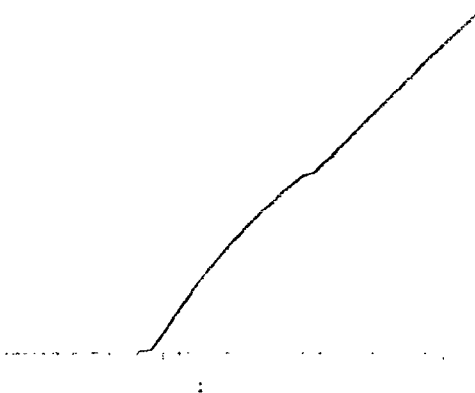
were fixed to the population mean estimates obtained from the Phase I model. Bayesian parameter estimation within NONMEM was then used to obtain individual predictions and parameter estimates.

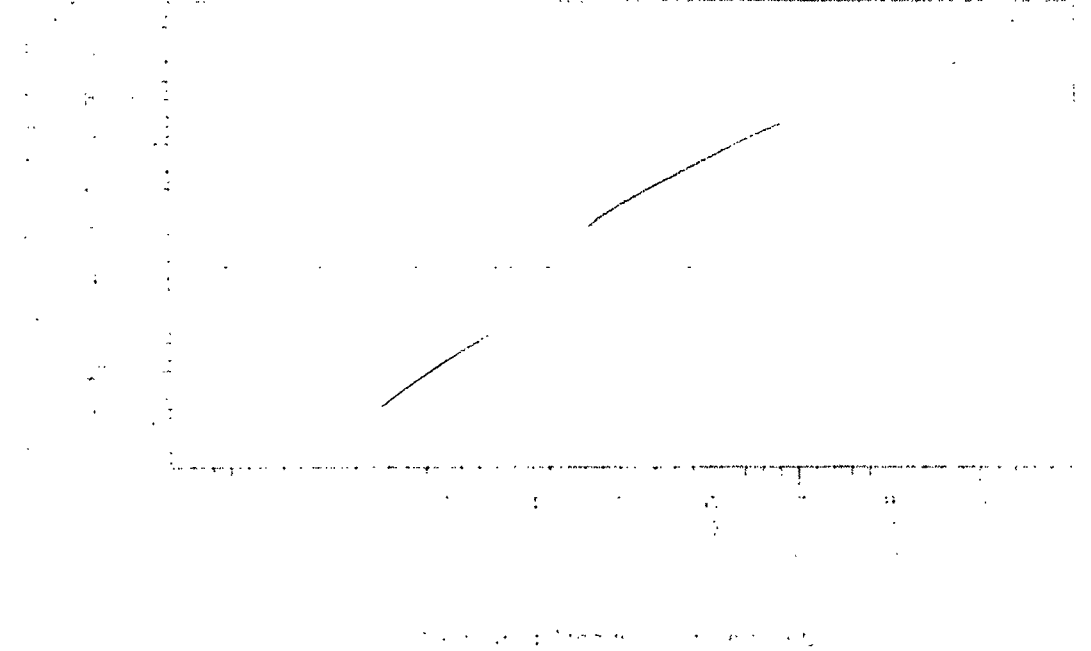
Reviewer's comment: Using the population mean estimates obtained from the Phase I (healthy subjects) model relied on the assumption that pharmacokinetics of atazanavir in HIV-1 infected patients is the same as that in healthy subjects. However, the pharmacokinetic data from A1424008 substudy indicated that Atazanavir (ATV) exposures are about 50% (geometric mean) lower in HIV-infected subjects as compared to healthy subjects under fed conditions. Therefore, this approach is not appropriate.

The applicant used Bayesian prediction only for generation of atazanavir exposures, and did not evaluate subject covariates. The applicant indicated that an evaluation of subject covariates on data with uncertainties pertaining to meal administration times may have led to false conclusions.

Pharmacokinetics Results for Phase II studies:

Scatterplots of the (population) predicted concentrations (based on population PK parameters) and individual predicted concentrations (based on individual PK parameters) versus measured concentrations are shown in the following figures.





The data showed, even when evaluating the individual predictions, model misfit can be observed. The above figures demonstrated that the model over-estimated at low concentrations and under-estimated at high concentrations. The applicant indicated that they were not able to improve the model fit primarily due to the large amount of variability coupled with the sparse sampling strategy.

We are not able to accept the population pharmacokinetic results, due to:

- uncertainty of the meal time relative to dosing
- all the PK parameter and inter- and intraindividual variability were fixed to the population mean estimates obtained from the Phase I (healthy subjects) model
- the concentrations estimated did not accurately predict the observed concentrations.

The simulated concentrations were used to compute estimates of individual subject AUC_{ss} (24hr), C_{max}, and C_{min} values. These estimated PK parameters were used to establish PK/PD relationships.

Pharmacodynamic: Since population PK analysis is not acceptable, the resulting PK/PD analysis is not acceptable either.

Interim Population PK/PD Analysis (A1424007) for Dose Selection: Steady state 24 h plasma concentration-time profiles from subjects who received 200, 400 or 600 mg of BMS-232632 in the fasted state, in an ascending multiple-dose safety/PK study (A1424002), were used to develop the population PK model.

Several structural models were fit to the data using NONMEM and goodness of fit was assessed to select an appropriate model. The selected model was a two-compartment

mixture model with two populations of K_a (absorption rate constant) and V_c (volume of the central compartment). The model resulted in half the population being classified as slow absorbers exhibiting a K_a (%SEM) of 1.45 1/h (24.2) compared to other half of the population of fast absorbers with a K_a of 6.48 1/h (50.5). Estimates of V_c (%SEM) in the two populations were 187 L (16.5) and 109 L (16.9). The mean (%SEM) clearance in the 200 mg once daily dose group (36.7 L/h (18.8)) was different from the 400 and 600 mg groups (25.5 L/h (7.2)). In addition, a mean (%SEM) absorption lag time was estimated as 0.47 h (1.4).

Reviewer's comment: The separation of these two groups was not based on any known covariates, and may not be valid.

Using the population PK model, Bayesian clearance estimates were obtained from each subject, which were used in conjunction with the subjectTM's dose to calculate an individual-specific steady state AUC. Logistic regression analyses were performed evaluating AUC as a predictor of failure to achieve a 1.5 log decrease in HIV RNA or probability of bilirubin elevation > 2.5 mg/dL.

Reviewer's comment: The interim population PK/PD analysis also assumed that pharmacokinetics of atazanavir in HIV-1 infected patients is the same as that in healthy subjects, which is not true. In addition, the interim analysis used fasted data to select the dose, but it is known that atazanavir exposure is higher after administered under fed conditions as compared to fasted conditions. Therefore, the results are not acceptable.

Conclusion: The results from population PK/PD analyses are not acceptable, and can not be used as a base for dose selection and labeling.

APPEARS THIS WAY
ON ORIGINAL

In vitro determination of human serum protein, albumin, and α -1-acid glycoprotein binding and blood cell distribution of BMS-232632
(MAP031/232632, Report 930000308)

The serum protein binding, human serum albumin (HSA) binding, and α -1-acid glycoprotein (AAG) binding of BMS-232632, and blood cell distribution of [14 C]BMS-232632 in humans were determined *in vitro* by equilibrium dialysis of spiked serum samples and incubation of spiked whole blood samples, respectively. Human serum, HSA, and AAG protein binding were determined in replicates of four by dialyzing serum against 0.134 M phosphate buffer (pH 7.4) at 37 °C for 6 h at 4 concentrations (serum) and one concentration (HSA and AAG). Blood cell distribution was determined by incubating [14 C]BMS-232632 at 37 °C in blood for 1 h at 3 concentrations, in triplicate. At the end of the experiment, aliquots of serum and buffer for protein binding were analyzed for BMS-232632 by a validated method. Aliquots of blood and plasma for blood cell distribution were measured for radioactivity by liquid scintillation counting. The mean (SD) results are summarized in the table below.

Concentration (ng/ml.)	Binding (%)			
	Serum Proteins	HSA	AAG	Blood Cells
100	82.8 (2.0)	-- ^a	-- ^a	31.5 (1.2)
1000	93.6 (0.4)	86.2 (4.7)	88.7 (3.9)	24.3 (1.2)
5000	88.8 (0.5)	-- ^a	-- ^a	-- ^a
10000	80.8 (1.4)	-- ^a	-- ^a	32.7 (4.3)
Overall Mean	86.5	--	--	29.5

^a Not determined

The free drug concentration ranged from 6.4 to 19.2% in human serum, which was comparable to HSA and AAG. The extent of protein binding and blood cell distribution did not depend on concentration over a 100-fold range. In conclusion, BMS-232632 is bound to human serum proteins (86.5%), albumin (86.2%), α -1-acid glycoprotein (88.7%), and red blood cells (29.5%).

930001292

TITLE: EVALUATION OF PERMEABILITY OF BMS-232632 THROUGH CACO-2 CELLS (32)

OBJECTIVES:

To determine the in vitro permeability of BMS-232632 across the Caco-2 cell monolayer and to predict the extent of absorption in humans after oral administration

METHODS:

Caco-2 cells (passage #17) were obtained from the _____ Inserts (surface area: 0.33 cm²) with a polycarbonate membrane (_____ pore size) were purchased from _____. Caco-2 cells were seeded onto a collagen coated polycarbonate filter membrane at a density of 80,000 cells/cm². The cells were grown in culture medium consisting of Dulbecco's modified Eagle's medium supplemented with 10% fetal bovine serum, 1% nonessential amino acids, 1% L-glutamine, 100 U/mL penicillin-G, and 100 µg/mL streptomycin. The culture medium was replaced every two days and the cells were maintained at 37°C, 95% relative humidity, and 5% CO₂.

Permeability studies were conducted with the monolayers cultured between 14 and 21 days, and the cell passage numbers were between 20 and 40. The transport medium was modified Hank's balanced salt solution (MHBS). The permeability studies were initiated by adding an appropriate volume of MHBS containing test compound to either the apical (apical to basolateral transport) or basolateral (basolateral to apical transport) side of the monolayer. Aliquots of 0.2 mL and 1.1 mL were placed in the apical and basolateral sides, respectively. The monolayers were placed on an orbital shaker (50 cycles/min) and incubated for 4 hours at 37°C. Samples were taken from both the apical and basolateral compartment at the end of the 4-hour period.

The concentrations of BMS-232632 were analyzed by a specific _____ assay.

Permeability coefficient (P_c) was calculated according to the following equation: $P_c = \frac{dA}{dt \cdot S \cdot C_0}$, where dA/dt is the flux of test compound across the monolayer (nmole/sec), S is the surface area of the cell monolayer (0.33 cm²), and C₀ is the initial concentration (µM) in the _____ donor compartment. The permeability coefficient values are expressed as nm/sec.

RESULTS:

At all apical pH tested, BMS-232632 had high P_c values (i.e., ≥100 nm/sec) that were comparable to drugs (e.g., metoprolol) that are completely absorbed in humans after oral administration. The basolateral to apical permeability (secretory direction) was greater (ca. 4-fold) than the apical to basolateral permeability (absorptive direction), suggesting that BMS-232632 may be a substrate of apically located efflux pumps (e.g., P-gp).

Table 1: Permeability of BMS-232632 across Caco-2 cell monolayer

	Apical to Basolateral P _e			Basolateral to Apical P _e		
	pm (%)			pm (%)		
Apical pH	5.5	6.5	7.4	5.5	6.5	7.4
Initial donor concentration of BMS-232632 (µM)	141	83	86	ND	86	ND
Replicate #1	114	99	99	ND	364	ND
Replicate #2	95	89	112		389	
Replicate #3	92	84	101		348	
mean ± SD	100 ± 12	90 ± 7	104 ± 7		367 ± 21	

Reference: Notebook A40647 page 53-91

ND: Not determined

CONCLUSIONS:

BMS-232632 had comparable absorptive permeability to drugs that are completely absorbed in humans. Additionally, it may be a substrate of efflux pumps (e.g., P-gp).

The study design and data analysis are acceptable.

COMMENT:

The initial donor concentrations of the test compound used in this study were very high. It may underestimate the B to A / A to B ratio by saturating possible efflux systems. Thus BMS-232632 is likely a more avid substrate of efflux systems than it appeared in this study.

930002892

TITLE: EVALUATION OF P-GLYCOPROTEIN INHIBITION BY BMS-232632 USING CACO-2 CELLS

OBJECTIVES:

To evaluate the P-glycoprotein inhibition potential of BMS-232632 using an in vitro digoxin (a P-gp substrate) inhibition model in Caco-2 cells.

METHODS:

Caco-2 cells (passage #17) were obtained from the _____ Inserts (surface area: 0.33 cm²) with a polycarbonate membrane (0.4 µm pore size) were purchased from _____. Caco-2 cells were seeded onto a collagen coated polycarbonate filter membrane at a density of 80,000 cells/cm². The cells were grown in culture medium consisting of Dulbecco's modified Eagle's medium supplemented with 10% fetal bovine serum, 1% nonessential amino acids, 1% L-glutamine, 100 U/mL penicillin-G, and 100 µg/mL streptomycin. The culture medium was replaced every two days and the cells were maintained at 37°C, 95% relative humidity, and 5% CO₂.

Permeability studies were conducted with the monolayers cultured for approximately 21 days, and the cell passage numbers were between 50 and 80. Both the apical to basolateral (A to B) transport as well as the basolateral transport (B to A) of [³H]-digoxin (specific activity: 37 Ci/mmol) were measured in the absence and presence of BMS-232632 (n=3). The transport medium was Hank™s balanced salt solution, pH 7.4, on both the apical and basolateral side. The concentration of digoxin used was 5 µM, and the concentrations of BMS-232632 used were 0.1, 1, 5, 10 and 50 µM. Verapamil, a P-gp inhibitor, was used as a positive control at a concentration of 10 µM. The studies were initiated by adding an appropriate volume of buffer containing digoxin to either the apical (for apical to basolateral transport) or basolateral (for basolateral to apical transport) side of the monolayer. The test compound, BMS-232632, was added to both sides of the monolayer. The monolayers were then incubated for 2 hours at 37°C. Samples were taken from either the apical (for basolateral to apical transport) or basolateral (for apical to basolateral transport) compartment at the end of the 2-hour period and analyzed for [³H]-digoxin using a radio-labeled liquid scintillation counter.

The apical to basolateral as well as the basolateral to apical permeability coefficient (P_c) of digoxin was calculated in the presence and absence of various concentrations of BMS-232632. Results are reported as percent inhibition of digoxin transport by BMS-232632. The IC₅₀ value was calculated using linear regression. Inhibition of digoxin transport by verapamil, a positive control, was also reported at a single concentration of 10 µM.

RESULTS:

BMS-232632 at the concentrations up to 10 µM showed weak inhibition of digoxin transport (<20%) and at 50 µM showed 87% inhibition. The inhibition value determined for verapamil (positive control) in this experiment was 63% at 10 µM. The IC₅₀ value for BMS-232632 was determined to be 28.7 µM.

Table 1: Percent Inhibition of Digoxin Transport in Caco-2 cells at Various Concentrations of BMS-232632

BMS-232632 Concentration (µM)	% Inhibition of Digoxin Transport
0.1	8.6
1	2.4
5	4.4
10	15.8
50	87.1

CONCLUSIONS:

BMS-232632 appears to be a weak inhibitor of P-gp with an IC₅₀ value of ~29 µM.

The study design and data analyses are acceptable.

930002701

TITLE: LIMITED EVALUATION OF CYP ENZYMES INVOLVED IN THE METABOLISM OF ATAZANAVIR (BMS-232632) IN HUMAN LIVER MICROSOMES

This report is a more detailed version of the human CYP enzyme inhibition study that is summarized in a one page report (Limited evaluation of the metabolism of BMS-232632 by rat, dog, and human liver microsomes and liver slices; identification of cytochrome P450s involved. Report no. 910065008)

OBJECTIVES:

To determine which CYP enzymes are involved in the metabolism of atazanavir in human liver microsomes, using specific chemical inhibitors for eight human CYP enzymes.

METHODS:

Human liver microsomes (5 subjects) were pooled for use in this study. These microsomal preparations had an average protein concentration of 24 mg/mL.

Incubations were conducted at 37°C for 10 min duration using a substrate concentration of 10 µM. Incubations were conducted in the presence of 0.5 mg/mL human liver microsomal protein, 50 mM potassium phosphate buffer (pH 7.4), and 1 mM NADPH. The addition of the cofactor NADPH started the reaction. Duplicate incubations were performed and the enzymatic activity terminated by the addition of an equal volume of acetonitrile. The concentrations of the various inhibitors were quinidine (CYP2D6, 15 µM), 4-methylpyrazole (CYP2E1, 20 µM), tranlylcypromine (CYP2C19, 30 µM), 8-methoxypsoralen (CYP2A6, 25 µM), sulfaphenazole (CYP2C9, 20 µM), and ketoconazole (CYP3A4, 20 µM). All of these inhibitors were dissolved in MeOH. A 2.5 µL portion of inhibitor solution was added to a 0.5 mL incubation. Inhibitor was pre-incubated with microsomes at 37°C for 5 min prior to the addition of atazanavir and NADPH. Immediately after the addition of NADPH, an aliquot was removed and dispensed directly into sample tube containing acetonitrile, and this sample served as a 0 hr control. Mechanism-based inhibitors were orphenadrine (CYP2B6, 100 µM), furafylline (CYP1A2, 20 µM), and troleandomycin (CYP3A4, 100 µM). All these inhibitors were dissolved in methanol, and a 2.5 µL portion of inhibitor solution was added to a 0.5 mL incubation. Inhibitor was pre-incubated with microsomes containing co-factors at 37°C for 15 min prior to the addition of atazanavir. Each 0.5 mL incubation was prepared by the addition of 0.312 mL of water, 0.1 mL 280 mM potassium phosphate buffer (pH 7.4), 0.01 mL human liver microsomes, 0.05 mL NADPH, 2.5 µL of inhibitor solution, and 25 µL of a 200 µM solution of atazanavir, which was in 10% acetonitrile in water. The total organic solvent in the incubations was 1%.

A 0.10-mL portion of the microsomal incubation supernatant, containing 50% acetonitrile, was mixed with 0.10 mL of water. The resulting 0.20 mL sample was injected into the _____ column.

The percent metabolism was calculated based on the ratio of peak areas of the total metabolite vs. the total drug related material from the UV chromatogram. In the _____ system used in this study, five metabolite peaks were used to calculate the total metabolite peak area. The rate of metabolism was calculated by converting the percent metabolism into moles of drug

consumed and then dividing by the time of incubation and amount of protein in the incubation. The percent inhibition was determined by dividing the difference between the rates for the solvent control and inhibited sample by the rate for the solvent control.

RESULTS:

The results suggest that CYP3A4 is the CYP enzyme responsible for the oxidation of BMS-232632 in human liver microsomes, as evidenced by the 100% and 71% inhibition by ketoconazole and troleandomycin, respectively (Table 1 and Figure 1). The production of all metabolites appears to be inhibited completely by the addition of ketoconazole and troleandomycin (except the carbamate hydrolysis metabolite being slightly less affected by troleandomycin). Additional evidence was provided in a correlation analysis relating the rates of oxidation of BMS-232632 and testosterone in human liver microsomes. The correlation between these two activities is highly significant ($r = 0.97$) which suggests that CYP3A4 metabolizes atazanavir (In vitro correlation of the oxidation of BMS-232632 and of testosterone in human liver microsomes: Report no. 910065007).

Addition of inhibitors for CYPs 1A2, 2A6, 2B6, 2D6, and 2E1 produced minor effects ranging from 0% to 16% inhibition as shown in Table 1 and Figure 1. These effects are judged to be not significant.

Inhibition results cannot be clearly assessed from the addition of sulfaphenazole, a CYP2C9 inhibitor and tranylcyromine, a CYP2C19 inhibitor, because they were co-eluted with several metabolites of BMS-232632. However, their effects on the remaining peaks in the metabolite profile were minimal. These peaks were produced at levels comparable to controls. These facts, along with the results found for CYP3A4, suggest that CYP2C9 and CYP2C19 are not significant enzymes in the metabolism of atazanavir.

However, there are some concerns with the design of the in vitro studies that complicate interpretation of the results. The investigators used a high concentration of ketoconazole (20 μM) in the in vitro incubations. At such a high concentration, ketoconazole inhibits other enzymes- there are reports that it may inhibit some of the CYP2C enzymes. Most laboratories use incubations with 1 μM or less of ketoconazole to determine whether a drug is metabolized by CYP3A4. Due to the problems with the CYP2C9 and CYP2C19 results discussed in the previous paragraph, we cannot rule out metabolism by those enzymes. The inhibition by troleandomycin is supportive of CYP3A4 involvement, but use of a high concentration of troleandomycin (100 μM) is not optimal. The high correlation with oxidation of testosterone is also supportive of CYP3A4 involvement, but correlation results are generally considered the weakest evidence and need to be supported by other studies (use of probe inhibitors, such as ketoconazole).

Table 1: Percent Inhibition of Metabolism of Atazanavir in Pooled Human Liver Microsomes in the Presence of Various Chemical Inhibitors Specific for Certain CYP Enzymes.

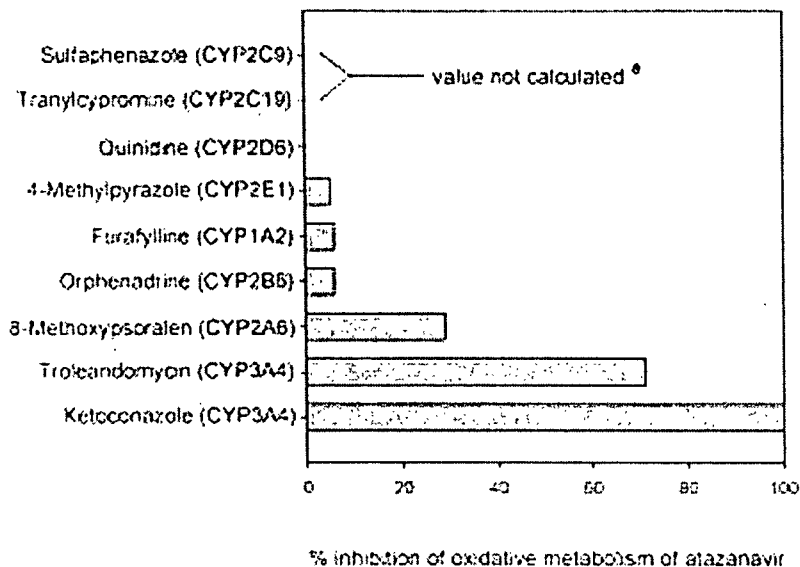
Inhibitor	Inhibitor concentration (µM)	CYP inhibited	rate, nmol/min/mg replicate A	rate, nmol/min/mg replicate B	average % inhibition
Direct Inhibitors					
Methylcoumatel ^a	-	-	0.13	0.13	-
Sulfaphenazole	20	2C9	0	0	0
Quinidine	15	2C8	0.13	0.13	0
1-Methylxanthine	20	2C1	0.17	0.15	5
Ketoconazole	20	3A4	0	0	100
Methylcoumatel ^a	-	-	0.14	0.15	-
1-Methylxanthine	25	2C1	0.11	0.11	16
Triacetylmure	30	2C19	0	0	0
Mechanism-based inhibitors					
Methylxanthol	-	-	0.13	0.17	-
Erythromycin	20	3A2	0.15	0.17	6
Clarithromycin	100	3A2	0.13	0.15	6
Ethacrynic acid	100	3A4	0.05	0.05	21

^a Inhibitor was present in two different test systems with different inhibitors.
^b Value could not be calculated since sulfaphenazole interfered with the latest eluting metabolic peak, but had no effect on earlier eluting peaks, which were produced at levels comparable to controls.
^c Value could not be calculated since triacetylmure interfered with 2 metabolic peaks, but had minimal effect on other peaks in the profile, which were produced at levels comparable to controls.

BEST POSSIBLE COPY

APPEARS THIS WAY
ON ORIGINAL

Figure 1: Percent Inhibition of Metabolism of Atazanavir in Pooled Human Liver Microsomes in the Presence of Various Chemical Inhibitors Specific for Certain CYP Enzymes.



* Value could not be calculated see Table I

CONCLUSIONS:

This study suggests that CYP3A4 is the enzyme responsible for the oxidative metabolism of atazanavir in human liver microsomes. However, several problems with the study design and results make this conclusion less than definitive. The results need to be interpreted in tandem with in vivo drug interaction and mass balance results.

COMMENT:

The sponsor may need to confirm the claim that CYP2C9 and CYP2C19 are not significant enzymes in the metabolism of atazanavir by using different CYP2C9 and CYP2C19 inhibitors which will not interfere with profiles of atazanavir metabolites. It would also be useful to repeat the ketoconazole evaluation with a lower concentration of ketoconazole.

910065054

TITLE: EVALUATION OF A NEW CHEMICAL ENTITY, CGP 73547 (BMS-232632), AS AN INHIBITOR OF HUMAN P450 ENZYMES

This study was conducted by _____

OBJECTIVES:

To evaluate the ability of BMS-232632 to inhibit the major P450 enzymes in human liver microsomes

METHODS:

The ability of BMS-232632 to inhibit the major P450 enzymes, namely, CYPs 1A2, 2A6, 2C8, 2C9, 2C19, 2D6, 2E1, 3A4/5 and 4A9/11, was examined with a pool of human liver microsomes (from 5 or more individuals). These microsomal samples were extensively characterized with respect to their P450 enzyme activity. To examine its ability to act as a reversible inhibitor, BMS-232632 was added to human liver microsomes together with each marker substrate. Incubations in duplicate were conducted at 37°C with NADPH. The concentrations of each marker substrate were Km/2, Km and 4Km. The concentrations of BMS-232632 were from 0.1 up to 3.0 µM. Incubations containing the organic solvent but no inhibitor were used as negative controls. Data were analyzed by Dixon plots to determine the type of inhibition and the inhibitory constant (Ki). To examine BMS-232632 as a mechanism-based inhibitor, human liver microsomes were pre-incubated in triplicate with BMS-232632 and NADPH for 10 min. After this 10-min pre-incubation period, an aliquot of microsomes was added to an incubation containing the marker substrate. The incubation was then carried out to measure the residual marker P450 activity.

CYP1A2 activity: 7-Ethoxyresorufin O-dealkylation. Incubations were conducted at 37°C for 2 min duration in the presence of 0.1 mg/mL human liver microsomal protein, 100 mM potassium phosphate buffer (pH 7.4) and 1 mM NADPH. α-Naphthoflavone and furafylline served as positive control.

CYP2A6 activity: Coumarin 7-hydroxylation. Incubations were conducted at 37°C for 10 min duration in the presence of 0.05 mg/mL human liver microsomal protein, 25 mM potassium phosphate buffer (pH 7.4) and 1 mM NADPH. Nicotine and 8-Methoxypsoralen served as positive control.

CYP2C9/10 activity: Tolbutamide hydroxylation. Incubations were conducted at 37°C for 60 min duration in the presence of 1 mg/mL human liver microsomal protein, 50 mM potassium phosphate buffer (pH 7.4) and 1 mM NADPH. Sulfaphenazole served as positive control.

CYP2C19 activity: S-Mephenytoin 4'-hydroxylation. Incubations were conducted at 37°C for 30 min duration in the presence of 1 mg/mL human liver microsomal protein, 50 mM potassium phosphate buffer (pH 7.4) and 1 mM NADPH. Hexobarbital or tranlycypromine served as positive control.

CYP2D6 activity: Dextromethorphan O-demethylation. Incubations were conducted at 37°C for 30 min duration in the presence of 1 mg/mL human liver microsomal protein, 100 mM potassium phosphate buffer (pH 7.4) and 1 mM NADPH. Quinidine served as positive control.

CYP2E1 activity: Chlorzoxazone 6-hydroxylation. Incubations were conducted at 37°C for 30 min duration in the presence of 0.5 mg/mL human liver microsomal protein, 50 mM potassium phosphate buffer (pH 7.4) and 1 mM NADPH. 4-Methylpyrazole served as positive control.

CYP3A4/5 activity: Testosterone oxidation. Incubations were conducted at 37°C for 8 min duration in the presence of 0.2 mg/mL human liver microsomal protein, 50 mM potassium phosphate buffer (pH 7.4) and 1 mM NADPH. Ketoconazole and troleandomycin served as positive control.

CYP4A9/11 activity: Lauric acid hydroxylation. Incubations were conducted at 37°C for 10 min duration in the presence of 0.4 mg/mL human liver microsomal protein, 50 mM potassium phosphate buffer (pH 7.4) and 1 mM NADPH.

RESULTS:

APPEARS THIS WAY
ON ORIGINAL

APPEARS THIS WAY
ON ORIGINAL

Table 1

Summary of the kinetic constants for various P450 enzyme activities

Enzyme	P450 Activity	Pre-determined Kinetic Constants ¹			Concentrations Studied (μM)
		Sample	K_m (μM)	V_{max} (pmol/min/mg)	
1A2	7-Ethoxycoumarin O-dealkylase	21	0.506	188	0.25, 0.50, 2.0
2A6	Coumarin 7-hydroxylase	17	0.715	2100	0.35, 0.70, 2.8
2C9	Tolbutamide methyl-hydroxylase	Pool of 7	360	397	100, 360, 1440
2C19	S-Mephenytoin 4'-hydroxylase	16	30.1	238	17.5, 35.0, 140
2D6	Dextromethorphan O-demethylase	14	4.60	780	2.5, 5.0, 20
2E1	Chlorzoxazone 6-hydroxylase	20	20.4	3550	15, 30, 120
3A4/5	Testosterone 6 β -hydroxylase	Pool of 7	55.8	4900	25, 50, 200
4A9/11	Lauroic Acid 12-hydroxylase	Pool of 7	15.4	1500	0.0, 15, 60

¹: These kinetic constants were determined previously (as a part of selecting the substrate concentrations used for this study) and formed the basis of

Table 2

Summary: Evaluation of CGP 73547 as a reversible and mechanism-based inhibitor of P450 enzymes in human liver microsomes

Concentrations of CGP 73547 studied: 0.1, 0.5, 1.0 and 3.0 μM

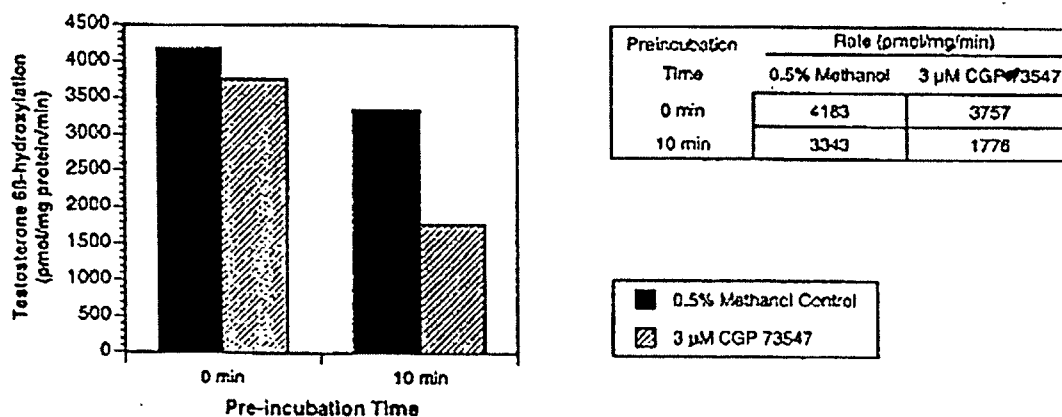
Enzyme	P450 Activity	Reversible (K _i value)	Mechanism-based
CYP1A2	7-Ethoxycoumarin O-dealkylase	~ 12.2 μM^{NCI}	No inhibition observed
CYP2A6	Coumarin 7-hydroxylase	*	No inhibition observed
CYP2C9	Tolbutamide methyl-hydroxylase	~ 12.2 μM^{CI}	No inhibition observed
CYP2C19	S-Mephenytoin 4'-hydroxylase	*	No inhibition observed
CYP2D6	Dextromethorphan O-demethylase	*	No inhibition observed
CYP2E1	Chlorzoxazone 6-hydroxylase	*	No inhibition observed
CYP3A4/5	Testosterone 6 β -hydroxylase	~ 2.35 μM^{CI}	Yes, inhibition observed
CYP4A9/11	Lauroic Acid 12-hydroxylase	*	No inhibition observed

*: Under the conditions examined, CGP 73547 did not inhibit these P450 enzymes. Therefore, the K_i value for inhibition of these P450 enzymes by CGP 73547 is greater than 3.0 μM , which is the highest concentration examined.

NCI: Non-competitive inhibition

CI: Competitive inhibition

Figure 1. Mechanism-based inhibition: CYP3A4/5



CONCLUSIONS:

The study results suggest that BMS-232632 is not a reversible inhibitor of CYP2A6, CYP2C19, CYP2D6, CYP2E1, and CYP4A9/11. However, it competitively inhibits CYP1A2, CYP2C9 and CYP3A4/5 with K_i values of 12.1, 12.7 and 2.35 μM , respectively. In addition, BMS-232632 is found to be a mechanism-based inhibitor to CYP3A4/5.

The study design and data analyses are acceptable.

NOTE:

Results from the study report no. 910073103, "Effects on cytochrome P450 3A4 activity in cultures of primary and immortalized human hepatocytes" further confirmed that BMS-232632 was an inhibitor to CYP3A4 and indicated that BMS-232632 was not an inducer for CYP3A4.

930000848

TITLE: A STUDY TO ASSESS THE POTENTIAL FOR INHIBITION OF HUMAN CYTOCHROME P450 BY ATAZANAVIR METABOLITES, BMS-421419 AND BMS-551160.

OBJECTIVES:

To determine the in vitro inhibitory activity of BMS-421419 and BMS-551160 on human cytochrome P450s.

METHODS:

The capacity of BMS-421419 and BMS-551160 to inhibit cDNA-derived cytochrome P450 enzymes in microsomes prepared from baculovirus-infected insect cells was measured using either 3-cyano-7-ethoxycoumarin (CYP1A2 and CYP2C19), 7-methoxy-

4-trifluoromethylcoumarin (CYP2C9) or 3-[2-(N, N-diethyl-N-methylamino)ethyl]-7-methoxy-4-methylcoumarin (CYP2D6) as substrates. CYP3A4 was tested with multiple substrates; 7-benzyloxy-4-trifluoromethylcoumarin and resorufin benzyl ether.

Assays were conducted in 96 well microtiter plates. The final concentrations of the substrates were chosen to be approximately the apparent K_m with the exception of 7-benzyloxy-4-trifluoromethylcoumarin, where the concentration chosen is below the apparent K_m . By definition, when the study is performed at the apparent K_m of the model substrate, the IC_{50} value is equal to two-times the K_i value. When the study is performed below the apparent K_m of the model substrate, the IC_{50} value approximates the K_i value.

The highest test substance concentration was 100 μM . After buffer, cofactors and test substance addition, the plates were pre-warmed to 37°C. Incubations were initiated by the addition of pre-warmed enzyme and substrate. For all enzymes except CYP2D6, the final cofactor concentrations were 1.3 mM NADP, 3.3 mM glucose-6-phosphate and 0.4 U/mL glucose-6-phosphate dehydrogenase. For CYP2D6, the final cofactor concentrations were 0.0081 mM NADP, 0.41 mM glucose-6-phosphate and 0.4 U/mL glucose-6-phosphate dehydrogenase. The final incubation volume was 0.2 mL. After 45-min incubation, reactions were stopped by the addition of 0.075 mL of 80% acetonitrile-20% 0.5M Tris base.

RESULTS:

IC_{50} values for the inhibition of human CYP isoforms are shown in Table 1. BMS-421419 did not inhibit any of the CYP isoforms investigated up to the highest concentration tested ($IC_{50} > 100 \mu M$). BMS-551160 inhibited CYP2C19 with an average IC_{50} value of 4.9 μM , and was a very weak inhibitor of CYP3A4 with average IC_{50} values of $>80 \mu M$. The compound did not inhibit CYP1A2, CYP2C9, and CYP2D6 up to the highest concentration tested ($IC_{50} > 100 \mu M$).

Table 1 Summary of IC_{50} Values (μM ; mean of three determinations)

Test Substance	CYP1A2	CYP2C9	CYP2C19	CYP2D6	CYP3A4 BFC	CYP3A4 BR
BMS-421419	>100	>100	>100	>100	>100	>100
BMS-551160	>100	>100	4.9	>100	82	86

CONCLUSIONS:

These in vitro results suggest that BMS-551160 but not BMS-421419 has the potential to alter the metabolic clearance of drugs that are highly metabolized by CYP2C19. The clinical significance of this result will depend on the plasma and/or hepatic concentrations of BMS-551160 achieved in vivo.

The study design and data analysis is acceptable.

920002969

TITLE: INHIBITION OF HUMAN CDNA-EXPRESSED UGT 1A1 BILIRUBIN GLUCURONIDATION ACTIVITY BY BMS-232632 AND INDINAVIR

This study was conducted by _____

OBJECTIVES:

To determine the potency of BMS-232632 and indinavir for the inhibition of human UGT 1A1 bilirubin glucuronidation activity.

METHODS:

Microsomes of lymphoblast cells heterologously expressing human UGT 1A1 were used for each experiment in this study.

Incubations were conducted at 37°C in a final volume of 0.2 ml in 50 mM sodium citrate buffer (pH 7.5) with 2 mM uridine diphosphoglucuronic acid (UDPGA), 27 µg/ml alamethicin, 10 mM MgCl₂, bilirubin and test compound. Bilirubin was dissolved in 100% DMSO and added to the incubation mix to the desired final bilirubin concentration. The final microsomal protein concentration was generally 1 mg/mL. Reactions were initiated by the addition of UGT enzyme. Termination of the reaction was achieved by the addition of 0.2 mL ethanol containing 2% ascorbic acid. For K_i determination, the test compound concentrations were 0, 3, 6, 12 and 24 µM. The bilirubin concentrations were 3, 6, 9, 12, and 15 µM. The incubation time was 38 minutes.

To determine K_i and inhibition mechanism, double reciprocal plots were constructed.

RESULTS:

BMS-232632 inhibits recombinant UGT 1A1 via a linear "mixed-type" mechanism with K_i of 1.9 µM.

Figure 1. The mixed-type kinetic mechanism

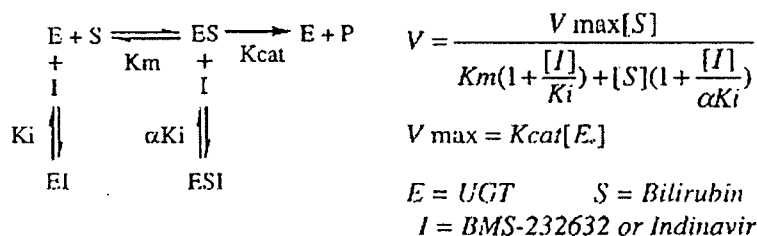


Table 1. Summary of the in vitro inhibition kinetics with BMS-232632 and indinavir

Compound	K_i (μM)	αK_i (μM)	Inhibition Mechanism	Inhibition at C_{ss} ⁴
BMS-232632 ¹	1.9	16.4 ($\alpha = 8.6$)	Linear Mixed	28.7%
Indinavir ²	47.9	1317 ($\alpha = 27.5$)	Linear Mixed ³	2.5%

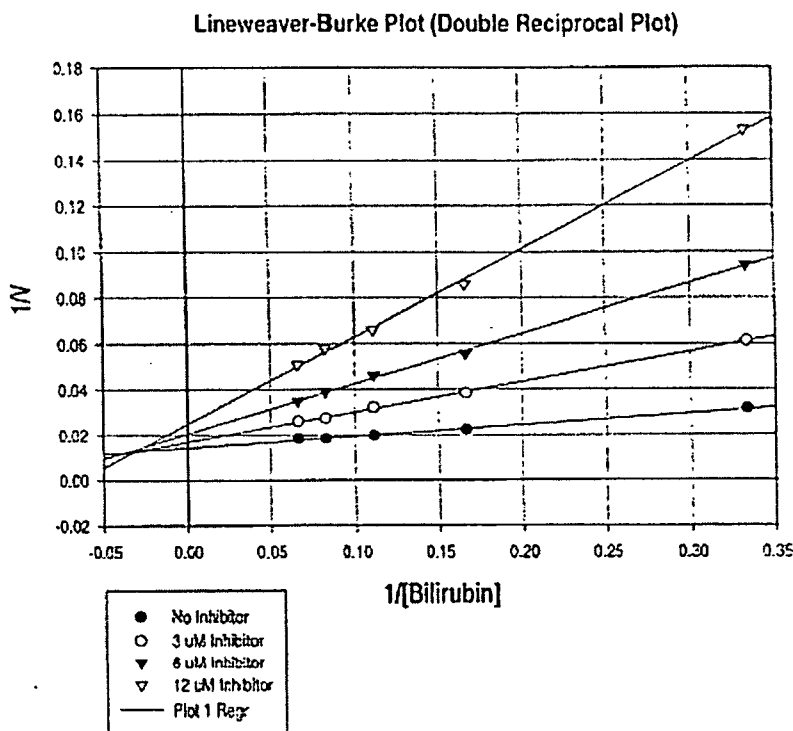
¹ UGT 1A1: $K_M = 4 \mu\text{M}$ and $V_{max} = 80 \text{ pmol/min mg protein}$ in this set of experiments.

² UGT 1A1: $K_M = 2.8 \mu\text{M}$ and $V_{max} = 62 \text{ pmol/min mg protein}$ in this set of experiments.

³ An uncompetitive mechanism with a $K_i = 100 \mu\text{M}$ was reported (FDA Summary Basis of Approval- indinavir).

⁴ For BMS-232632, $C_{ss} = 1.73 \mu\text{M}$ (Study A1424-013, 400 mg QD); for indinavir, $C_{ss} = 3.84 \mu\text{M}$ (Crixivan package insert, 800 mg TID); [Bilirubin] = $6.84 \mu\text{M}$.

Figure 2. Double reciprocal plots of concentration dependence of bilirubin glucuronidation in presence of fixed concentrations of BMS-232632 (inhibitor)



CONCLUSIONS:

BMS-232632 appears to be a more potent inhibitor of UGT 1A1 in vitro than indinavir. The study design and data analyses are acceptable.

920007575

TITLE: INHIBITION OF BILIRUBIN GLUCURONIDATION IN HUMAN LIVER
MICROSOMES AND CDNA-EXPRESSED UGT 1A1 BY BMS-232632, INDINAVIR,
SAQUINAVIR AND NELFINAVIR

This study was conducted by _____.

OBJECTIVES:

To compare the potency of BMS-232632 for the inhibition of human UGT 1A1 bilirubin glucuronidation activity with other HIV-protease inhibitors (indinavir, saquinavir and nelfinavir)

METHODS:

The potency of BMS-232632 for the inhibition of bilirubin glucuronidation was tested against the potency of other HIV-protease inhibitors, i.e. indinavir, nelfinavir and saquinavir. IC_{50} values were determined for each test compound using both pooled HLM and cDNA-expressed human UGT1A1. The bilirubin concentration was 5 μ M, which is approximately equal to the K_m value for bilirubin glucuronidation in both HLM and cDNA-expressed UGT1A1. A total of 9 inhibitor concentrations were used, ranging from 0.03 to 300 μ M.

Incubations were conducted at 37°C in a final volume of 0.2 mL in 50 mM sodium citrate buffer (pH 7.5) with 2 mM uridine diphosphoglucuronic acid (UDPGA), 27 μ g/mL alamethicin, 10 mM $MgCl_2$, bilirubin and test compound. Bilirubin was dissolved in 100% DMSO, and added to the incubation mix to achieve a final bilirubin concentration of 5 μ M. Reactions were initiated by the addition of HLM or expressed UGT enzyme. Termination of the reaction was achieved by the addition of 0.2 mL ethanol containing 2% ascorbic acid.

IC_{50} determinations were carried out using the incubation conditions described above. The test substance concentrations were as follows: 0 (solvent only), 0.03, 0.1, 0.3, 1, 3, 10, 30, 100, and 300 μ M. Control incubations (without test substance) contained equal amounts of solvent vehicle (methanol) as the incubations containing test substance. For cDNA-expressed UGT 1A1, the assay time was 24 min, and the final protein concentration was 0.5 mg/mL. The assay time for HLM incubations was 12 min, and the final protein concentration was 0.125 mg/mL.

RESULTS:

Table 1. IC₅₀ values for the inhibition of bilirubin glucuronidation by HIV-protease inhibitors in vitro

Compound	IC ₅₀ Values (μM)	
	UGT-1A1	HLM
BMS-232632	2.4	2.5
Indinavir	87	68
Saquinavir	7.3	5.0
Nelfinavir	8.4	2.7

Table 2. Steady-state plasma concentrations and protein binding of protease inhibitors

Drug	Dose	C _{max} (μM)	C _{ss} (μM)	Plasma Protein Binding (%)	Unbound C _{max} (μM)	Unbound C _{ss} (μM)
BMS-232632 ^a	400 mg QD	7.63	1.73	86.5 ^b	1.03	0.23
Indinavir ^c	800 mg TID	12.6	3.84	60 ^c	5.04	1.54
Saquinavir ^{d, e}	600 mg TID	0.38	0.21	98 ^f	0.008	0.004
Nelfinavir ^{g, h}	750 mg TID	6.6	4.40	>98 ^h	<0.132	<0.09

^a AI424-013 (BMS-232632-ketoconazole interaction study)

^b Data on file

^c Crixivan (indinavir) package insert

^d C. Merry *et al.* AIDS 11: F117-F120, 1997

^e J.F. Bergmann *et al.* Fundam. Clin. Pharmacol. 13: 352, 1999

^f Fortavase (saquinavir) package insert

^g C. Merry *et al.* AIDS 12: 1163-1167, 1998

^h Viracept (nelfinavir) package insert

CONCLUSIONS:

Considering the extent of plasma protein binding and the consequent unbound steady-state plasma concentrations attained after therapeutic doses of these four protease inhibitors, BMS-232632 appears to be the most potent UGT 1A1 inhibitor in vivo among these four HIV-protease inhibitors (Its IC₅₀ value is only 2-fold higher than the unbound C_{max} value). The concentrations after therapeutic doses of BMS-232632 may be high enough to lead to significant inhibition of UGT 1A1 in vivo, and hence, the observed hyperbilirubinemia.

The study design and data analyses are acceptable.

930000864

TITLE: BIOTRANSFORMATION OF [14 C] BMS-232632 AFTER ORAL ADMINISTRATION TO RATS, DOGS AND HUMANS

This review focused on results from the study in humans

OBJECTIVES:

To compare the biotransformation profiles in plasma, urine, bile and feces and to determine the nature and the extent of the biotransformation of BMS-232632 in rats, dogs and humans.

METHODS:

Urine, feces, and plasma samples were obtained from three disposition studies following the administration of [14 C] BMS-232632 to rats, dogs, and humans. In vivo studies were conducted using a mixture of two radiolabeled forms of [14 C] BMS-232632. In the human study AI424-029, plasma (1, 3 and 8 h), urine, and feces were obtained from 2 groups (n= 8, 3) of healthy male subjects administered single 400-mg oral doses (100 μ Ci). A second group of human subjects (n=3) was dosed because of lower than desired recovery of radioactivity in urine and feces from the group of eight subjects.

— analysis of biological samples:

Each pooled urine sample from humans (1 mL) was evaporated to dryness under nitrogen and redissolved in — mobile phase solvent A containing 10% acetonitrile. Each sample was spiked with 2 μ L of an acetonitrile solution containing reference standard BMS-232632 and, if available, BMS-421419. These samples were centrifuged for 1 min at 14,000 rpm and 200 μ L of supernatant were injected into the —. Each pooled plasma sample (1 mL) was extracted by addition of 2 volumes of acetonitrile to 1 volume of plasma. After centrifugation of the acetonitrile/water mixture at 2500 rpm for 10 min, the supernatant fraction was removed and saved, and the precipitate was resuspended and vortexed in acetonitrile/water (2:1, v/v). Following centrifugation, the supernatant fraction was removed and combined with the first supernatant. The second extraction was repeated. The combined supernatant fraction was evaporated to dryness under nitrogen. The evaporated samples from humans were reconstituted in — of mobile phase solvent A containing 10% acetonitrile. Each sample was spiked with 2 μ L of acetonitrile solution containing reference standard BMS-232632 and, if available, BMS-421419. Following centrifugation at 14,000 rpm for 1 min, a 100 or 200 μ L portion was injected into the —. Each pooled fecal homogenate sample (~ 1.0 g) was extracted by addition of 2 volumes of acetonitrile. The mixture was sonicated for 5 min and then shaken mechanically for 20 min. After centrifugation of the acetonitrile/water mixture at 2500 rpm for 10 min, the supernatant fraction was removed and saved, and the precipitate was resuspended and vortexed in acetonitrile/water (2:1, v/v). Following centrifugation, the supernatant was removed and combined with the first supernatant. The second extraction was repeated. The volume of supernatant used for analysis in the human was 0.5 mL. This combined supernatant was evaporated to dryness under nitrogen. The evaporated samples from humans were reconstituted in 0.45 mL of mobile phase containing 10% acetonitrile. Each sample was spiked with 2 μ L of an acetonitrile solution containing reference standard BMS-232632 and, if available,

BMS-421419. Following centrifugation at 14,000 rpm for 1 min, a 100 μ L portion was injected into the _____

_____ was performed on a _____ equipped with a photodiode array ultraviolet detector. A _____ column _____ was used. The mobile phase flow rate was 0.25 mL/min. Besides using the diode array detector to help determine metabolite peaks of interest, a radioactivity profile was obtained during some _____ inserted after the photodiode array detector. The _____ effluent was _____ approximately _____ half of the flow was introduced into the _____ and the other half of the effluent was collected during 0.25 or 0.5 min intervals using a _____ fraction collector. Radioactivity in these fractions of column eluate was determined by the addition of 5 mL of _____ and by use of a _____ analyzer or by first collecting column _____

RESULTS:

In human plasma at 3 and 8 h, BMS-232632 accounted for 46.5 to 64.3% of the plasma radioactivity for both groups (Sub 10-12 and Sub 1-8). This was slightly higher than the percentages seen in rats and dogs at similar time points. Plasma profiles from the two subject groups were similar. BMS-421419, BMS-551160 and a keto metabolite (M41) each constituted approximately 10% of the plasma radioactivity at 3 h and slightly higher at 8 h. Monohydroxylated metabolites (M33, M34, M36), carbamate-hydrolyzed metabolites (M23, M24) and a keto metabolite (M40) were all minor components constituting less than 4% of the plasma radioactivity. All of the human plasma metabolites were present in the plasma of one or more of the animal species. BMS-421419 and BMS-551160 have been tested for anti-HIV activity and CYP P450 inhibition. These circulating metabolites lacked anti-HIV activity and BMS-421419 demonstrated no CYP P450 inhibition. BMS-551160 showed no inhibitory effect on CYP1A2, CYP2C9, CYP3A4 and CYP2D6 with IC50 results that ranged from 82 to greater than 100 μ M. The IC50 value for CYP2C19 was 4.9 μ M. The keto metabolite (M41) could not be generated using an immortalized human hepatocyte bioreactor or fungal incubations for further identification and activity testing.

Humans excreted 13% and 9% of the dose in the urine for subjects 10-12 and 1-8, respectively. The urinary profiles were similar for subjects 10-12 and subjects 1-8. BMS-232632 accounted for 43.8 and 36.7% of the urinary radioactivity for both groups (Sub 10-12 and Sub 1-8, respectively). This was higher than the percentages seen in rat and dog urine. The human urine (Sub 10-12) also contained BMS-421419 (5.3%), BMS-421419 glucuronide (9.4%), dihydroxylated metabolites M21 and M29 (0.8 and 6.2%, respectively), and at least three monohydroxylated metabolites M33, M34 and M36 (4.6% combined).

Humans excreted 79 and 56% of the dose in the feces for subjects 10-12 and 1-8, respectively. Human feces contained BMS-232632 (15.0% of the fecal radioactivity), at least 3 monohydroxylated metabolites M33, M34 and M36 (31.5% combined), and dihydroxylated metabolites M20, M26, M29 and M31 (25.7% combined). The rat fecal profiles, rat biliary profiles and the overall similarity between the biotransformation in rats and humans argue that human bile might also contain glucuronides, which may be hydrolyzed by intestinal microflora, and therefore are not present in human feces.

6.2 Filing and Review Form

Office of Clinical Pharmacology and Biopharmaceutics				
New Drug Application Filing and Review Form				
General Information About the Submission				
Information		Information		
NDA Number	021567	Brand Name	Reyataz	
OCPB Division (I, II, III)	III	Generic Name	Atazanavir	
Medical Division	530	Drug Class	Protease inhibitor	
OCPB Reviewer	Jenny H. Zheng and Derek Zhang	Indication(s)	Treatment of HIV infection	
OCPB Team Leader	Kellie Reynolds	Dosage Form	100/150/200 mg capsule	
Date of Submission		Dosing Regimen	400 mg QD	
Estimated Due Date of OCPB Review		Route of Administration	Oral	
PDUFA Due Date	6/20/03	Sponsor	Bristol-Myers Squibb Company	
Division Due Date		Priority Classification	Priority	
Clin. Pharm. and Biopharm. Information				
	"X" if included at filing	Number of studies submitted	Number of studies reviewed	Critical Comments If any
STUDY TYPE				
Table of Contents present and sufficient to locate reports, tables, data, etc.	x			
Tabular Listing of All Human Studies	x			
HPK Summary	x			
Labeling	x			
Reference Bioanalytical and Analytical Methods	x			
I. Clinical Pharmacology				
Mass balance:	x	1	1	029
Isozyme characterization:	x	11	7	MAP001, 910065008, MAP048, 910064951, 910064948, 910065007, XT042496, 98904, MAP036, MAP178, MAP022
Blood/plasma ratio:	x	1	1	MAP031
Plasma protein binding:	x	1	1	MAP021, MAP031
Pharmacokinetics (e.g., Phase I) -				
Healthy Volunteers-				
single dose:	x	1	1	001
multiple dose:	x	4	4	002,040, 011, 076
Patients-				
single dose:	x			007, 008, 009
multiple dose:	x	3	3	007, 008, 009
Dose proportionality -				
fasting / non-fasting single dose:	x			001
fasting / non-fasting multiple dose:	x			011
Drug-drug interaction studies -				
In-vivo effects on primary drug:	x	15	14	004, 012, 013, 016, 021, 027, 028, 033, 039, 055, 056, 057, 058, 030, 051
In-vivo effects of primary drug:	x			004, 012, 016, 027, 028, 033, 055, 056, 057, 058, 030
In-vitro:				
Subpopulation studies -				
ethnicity:				
gender:	x	1	1	014
pediatrics:	x	1		Insufficient data
geriatrics:	x			014
renal impairment:				
hepatic impairment:	x	1	1	015

PD:				
Phase 2:	x			007,008
Phase 3:				045, 034, 043? Data not submitted yet
PK/PD:				
Phase 1 and/or 2, proof of concept:	x			007,008, 076
Phase 3 clinical trial:				045, 034, 043? Data not submitted yet
Population Analyses -				
Data rich:				
Data sparse:	x	3	3	007, 930002915, 930002847
II. Biopharmaceutics				
Absolute bioavailability:				
Relative bioavailability -				
solution as reference:				
alternate formulation as reference:	x	3	1	005, 010, 025
Bioequivalence studies -				
traditional design; single / multi dose:				
replicate design; single / multi dose:				
Food-drug interaction studies:	x	1	1	003
Dissolution:	x	1	1	
(IVIVC):				
Bio-wavier request based on BCS				
BCS class				
III. Other CPB Studies				
Genotype/phenotype studies:				
Chronopharmacokinetics				
Pediatric development plan	x	1		020
Penetration	x	1		MAP037
Literature References				
Total Number of Studies		49	40	
Filability and QBR comments				
	"X" if yes	Comments		
Application filable ?	x	Reasons if the application is <u>not</u> filable (or an attachment if applicable) For example, is clinical formulation the same as the to-be-marketed one?		
Comments sent to firm?		Comments have been sent to firm (or attachment included). FDA letter date if applicable.		
QBR questions (key issues to be considered)				
Other comments or information not included above				
Primary reviewer Signature and Date				
Secondary reviewer Signature and Date				

CC: NDA 21-567, HFD-850(P. Lee), HFD-860 (M. Mehta), HFD-530(V. Reddy), HFD-880(K. Reynolds, J. Lazor, A. Selen), CDR

**This is a representation of an electronic record that was signed electronically and
this page is the manifestation of the electronic signature.**

/s/

• Jenny H. Zheng
6/20/03 04:03:00 PM
BIOPHARMACEUTICS

Derek Zhang
6/20/03 04:10:05 PM
BIOPHARMACEUTICS

Kellie Reynolds
6/20/03 04:27:24 PM
BIOPHARMACEUTICS